Spring 5-9-2010

# Microwave Spectroscopy and Structures of Several Substituted Acetylenes and Fluorocarbons

Joseph A. Fournier
*University of Connecticut - Storrs*, jfournier@ct.metrocast.net

# Microwave Spectroscopy and Structures of Several Substituted Acetylenes and Fluorocarbons

Joseph A. Fournier
Department of Chemistry
University of Connecticut, Storrs, CT

# Table of Contents

## Abstract

Several substituted acetylene compounds and several fluorocarbons have been studied and analyzed by their microwave rotational spectra and the structures characterized. Simple hydrocarbons exhibit staggered structures with dihedral angles anti ($180^o$) or gauche ($\pm 60^o$) from the eclipsed position. These structures result from steric repulsive interactions between alkyl groups. Alkyl groups separated by distances longer than the sum of their van der Waals radii are weakly attractive via dispersion interactions. A microwave study of 6-methyl-3-heptyne, which can be thought of as an ethyl group separated from an isobutyl group by a C≡C spacer, revealed two structures each with the ethyl and isobutyl groups eclipsed. The isobutyl group can exist in two conformers of $C_1$ and $C_s$ symmetry, and both have been observed and assigned. To complement this study, the compound 2-methylpentane was analyzed. 2-Methylpentane is 6-methyl-3-heptyne without the C≡C spacer. Three conformers were observed and assigned, each exhibiting staggered structures. These two studies show that interactions depend on distance. At short distances, steric repulsions dominate leading to staggered structures. Dispersion attractions dominate at longer distances, giving rise to eclipsed structures.

The structure of 3,5-octadiyne is currently under investigation. This compound is equivalent to two ethyl groups separated by two C≡C spacers. The structure of 3-hexyne, which has one such spacer, was previously determined to be eclipsed ($C_{2v}$) and computational studies show the barrier to internal rotation to be only about 30 cal/mol. The goal of this study is to determine if these weak dispersion attractions still dominate at longer distances. Extensive quantum chemical computations are complete and predict an extremely flat potential surface with an essentially zero barrier. The microwave experiments have been quite difficult. If eclipsed $C_{2v}$, the microwave spectrum is expected to be relatively simple. The staggered $C_{2h}$ form would not be observable due to the absence of a dipole moment. A family of nine lines has been observed with near equal spacing, consistent with a symmetric top. It is thought that these lines may result from free rotation of the ethyl end groups, which would mean that the weak dispersion attractions between the end groups are too weak at these longer distances. More work is required to confirm this hypothesis.

The structure of the polymer polytetrafluoroethylene (Teflon©) is known to be helical. Numerous computational studies on shorter perfluoroalkane oligomers have been performed, but few experiments have been conducted. The microwave spectra of perfluoropropane, perfluoropentane, and perfluorohexane have been observed and assigned. The structures of perfluoropentane and –hexane were determined to be helical with a CCCC dihedral angle of about $17^o$ away from trans, in good agreement with the dihedral angle in Teflon. Perfluoropropane, however, was found to be non-helical. The steric and dipole interactions between F atoms that have been attributed to the helicity of Teflon appear to be insufficient in a three carbon chain to cause a twist in the structure. The gauche and trans conformers of 1H-heptafluoropropane have also been assigned and characterized. The trans form, like perfluoropropane, is also non-helical.

# Chapter 1. Introduction to Microwave Spectroscopy

## Theoretical

The various energy levels of atoms and molecules are discrete, a consequence of the laws of quantum mechanics. Atoms and molecules can be excited from a lower energy state to a higher one using electromagnetic radiation with energy equal to the energy difference between the two states. Once excited, the atoms or molecules will fall back to the original energy state, releasing electromagnetic radiation of equal energy. Detection and analysis of this radiation allows for the determination of structural and energy dynamics of a molecule.

Most simple organic molecules have rotational energy states in the microwave region of the electromagnetic spectrum (1-100 GHz). Rotation of any rigid body is based on the moments of inertia about the center of mass. The moment of inertia about the x-axis, $I_{xx}$, is equal to the sum of the mass of all atoms multiplied by the distance from the x-axis squared:

$$I_{xx} = \sum m_i(y_i + z_i)^2$$

The moments of inertia about the y and z axes are similarly defined. The moments of inertia can be arranged into the following matrix:

$$\begin{pmatrix} I_{xx} & I_{xy} & I_{xz} \\ I_{yx} & I_{yy} & I_{yz} \\ I_{zx} & I_{zy} & I_{zz} \end{pmatrix}$$

where the off-diagonal elements are called the products of inertia and are defined as follows:

$$I_{xy} = I_{yx} = -\sum m_i x_i y_i$$
$$I_{xz} = I_{zx} = -\sum m_i x_i z_i$$
$$I_{yz} = I_{zy} = -\sum m_i y_i z_i$$

The matrix can be diagonalized to give:

$$\begin{pmatrix} I_a & 0 & 0 \\ 0 & I_b & 0 \\ 0 & 0 & I_c \end{pmatrix}$$

When this is performed the x,y,z set of coordinates is transformed to a set of mutually perpendicular axes a,b,c called the principal axes. The diagonal elements of the moment of inertia tensor are now principal moments of inertia $I_a$, $I_b$, $I_c$ such that $I_a \leq I_b \leq I_c$. By use of quantum mechanical laws, it can be shown that the rotational energy levels of molecules are related to the inverses of the principal moments of inertia. These rotational levels are determined by the three rotational constants A, B, C. The rotational constants are defined as:

$$A = h / 8\pi^2 I_a = 505379.05 / I_a \quad \text{(where A is in units of MHz and } I_a \text{ is in u}\text{Å}^2\text{)}$$

where h is Planck's constant. B and C are similarly defined, such that $A \geq B \geq C$. From these rotational constants the microwave, or rotational, spectrum of a molecule can be determined.

Since the moments of inertia depend on the identity and positions of each atom in a molecule, the various possible structures of a single molecule (called conformations) give unique microwave spectra. Thus, the assignment of a microwave spectrum to rotational transitions allows for the determination of the stable conformations of a particular molecule. Furthermore, since the moments of inertia also depend on the bond lengths, bond angles, and dihedral angles between atoms in a molecule, the microwave spectrum can also aid in determining the structural details of the conformations.

**Experimental**

Microwave spectroscopy is carried out on molecules in the gas phase, as collisions in a condensed phase quickly relax the molecules back to the ground rotational state. Collisions are still frequent in the gas phase at room temperature and pressure, therefore, microwave spectroscopy must be performed at very low temperatures and pressures (~ $10^{-6}$ atm). The standard protocol is to distill vapor of the sample into a stainless steel tank. A carrier gas (typically He, Ne, or Ar) is added to give a sample mixture of ~ 1%. The carrier gas has no net dipole moment and, thus, does not interact with microwave radiation. The sample is fed into the microwave spectrometer between

0.5 – 3 atm of pressure. Since the sample is traveling from room pressure to very low pressure, supersonic expansion occurs upon entrance into the spectrometer. The expansion creates a "molecular beam" such that collisions between molecules are greatly reduced. The expansion, as well as collisions with the carrier gas, drastically cools the sample to an estimated 2-3 K. The cold temperatures relax and "lock" the molecules into their lowest energy structures.

Gas pulses are introduced into the spectrometer at a frequency of 5 Hz and five microwave pulses are observed per gas pulse. The frequency of choice is entered into a computer work station and mirrors inside the spectrometer cavity are adjusted to create a resonant frequency. The signal is detected as a free induction decay and transformed (Fourier transform) into a frequency signal on the computer work station. If the molecule does not have a rotational transition at a certain frequency, only background noise is observed. When there is a rotational transition, the molecules will absorb the microwave radiation. This radiation is released upon relaxation back to the original state and is detected. A transition signal is displayed as a pair of sharp peaks due to the Doppler effect. The capable frequency range of a microwave spectrometer is typically from 5 – 20 GHz. The uncertainty of transition measurements is estimated to be about 2 kHz.

**Data Analysis**

Molecular model calculations are first made using various computer programs, where the molecule of interest is "built" through approximate mass, bond length, bond angle, and dihedral angle inputs. From these structures, the moments of inertia about the three principal axes are calculated. The three rotational constants are then determined and used to predict the rotational spectra. Model spectra may not be quantitatively accurate, but the predicted patterns are reliable in assigning conformations. Once transitions are observed, they must then be assigned to the set of quantum numbers which describe the transition from the lower rotational state to a higher state. If the original model is accurate enough, the observed lines might easily be "matched" to the predicted transitions. Calculations would prove an assignment to be correct or not. Spectral fitting

programs, such as jb95, have become invaluable tools to help assign conformations. Once assigned, the experimental rotational constants are calculated. To improve the fits, centrifugal distortion constants are included in the calculations. Rigid molecules have fewer centrifugal distortion constants with relatively small values. More floppy molecules require more distortion constants with larger values. *Ab initio* quantum mechanical calculations are usually performed to interpret the structure and to estimate the relative energies of the observed conformations.

# Chapter 2. Structures of Two Conformers of 6-methyl-3-heptyne and Three of 2-methylpentane

## Introduction

Alkanes exhibit conformations with dihedral angles 180° or ± 60° from the syn-eclipsed position. The insertion of a C≡C spacer between the alkyl groups changes the most stable form to syn-eclipsed. This is consistent with the model that the dominant interaction between the alkyl groups is the weak nonbonded dispersion attraction, since the groups are separated by distances longer than the sum of their van der Waals radii. This has been demonstrated in the microwave studies of 3-hexyne[1] ($CH_3CH_2C{\equiv}CCH_2CH_3$), where the structure was determined to have syn-eclipsed $C_{2v}$ symmetry, and of 3-heptyne[2] ($CH_3CH_2C{\equiv}CCH_2CH_2CH_3$). In the case of 3-heptyne, the propyl group exists in anti and gauche conformations. In the anti form, the ethyl and propyl end groups are strictly syn-eclipsed ($C_s$). The ethyl group approximately eclipses the "center of electron density" of the opposing propyl group in the gauche conformation.

Extensive quantum mechanical calculations were carried out on 3-hexyne.[3] The computations did not agree with the experimentally determined $C_{2v}$ structure until very large basis sets were used. DFT methods were unsuccessful because they do not include dispersion interactions. HF calculation predict the $C_{2v}$ form only at the HF/aug-cc-pVQZ//(VTZ) level of theory. MP2 calculations at the same basis set predict a $C_{2v}$ structure with a torsional barrier of ~20 cal/mol, a very flat barrier.

To continue characterization of substituted acetylene compounds and analysis of the dispersion attractions, the microwave spectrum of 6-methyl-3-heptyne ($CH_3CH_2C{\equiv}CCH_2CH(CH_3)_2$, MHept) has been observed and assigned. This compound is analogous to 3-heptyne with one end group changed from propyl to isobutyl. Recently, analysis of a benchmark compound 4-methyl-1-pentyne[4] ($HC{\equiv}CCH_2CH(CH_3)_2$) was performed. The isobutyl group of MHept is expected to exist in gauche and anti conformations as it does in 4-methyl-1-pentyne (Figure 1). The rotational microwave spectra of both conformers have been assigned and the inertial constants analyzed to determine the dihedral angles between the ethyl and isobutyl groups. In addition, a second benchmark compound 2-methylpentane ($CH_3CH_2CH_2CH(CH_3)_2$, MPane), which is MHept without the C≡C spacer, is analyzed. MPane is more complicated than MHept due to differences in the torsional barriers. In MHept, a single conformer about the $–CH_2C{\equiv}CCH_2–$ axis is expected because the torsional barrier is so small. In MPane, there is a substantial ethane-like torsional barrier, $-CH_2-CH_2-$, supporting both anti and gauche conformations. As a result, AA(anti-anti), AG(anti-gauche), GA, GG(cis), and GG(trans) are possible conformations about the $C_4$-$C_3$ and $C_3$-$C_2$ bonds in MPane (see Figure 2). The first conformer label designates the conformation of the $C_5$-$C_4$-$C_3$-$C_2$ chain and the second designates the $C_4$-$C_3$-$C_2$-$H_{14}$ chain. The GG(trans) and GA conformers have unfavorable 1-3 methyl-methyl steric interactions and were not observed.

Figure 1. 6-methyl-3-heptyne with the expected symmetrical $C_s$ (left) and asymmetrical $C_1$ (right) conformations of the isobutyl group.

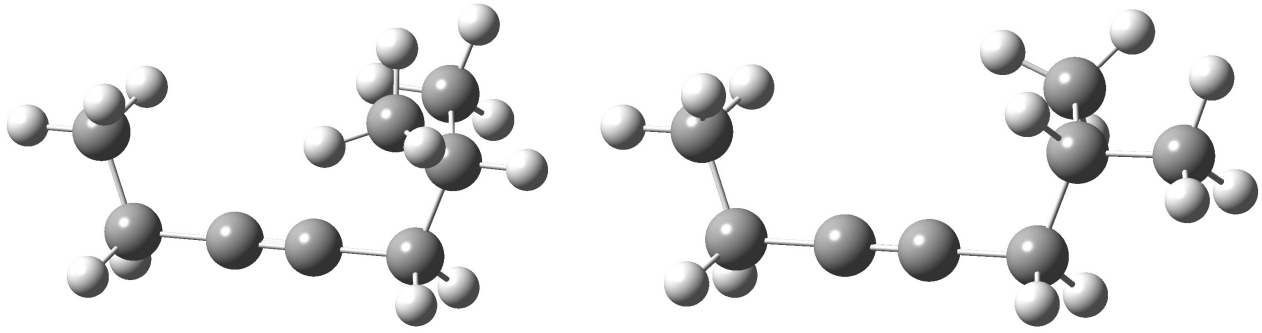

Figure 2. Models of the five possible conformations of 2-methylpentane.

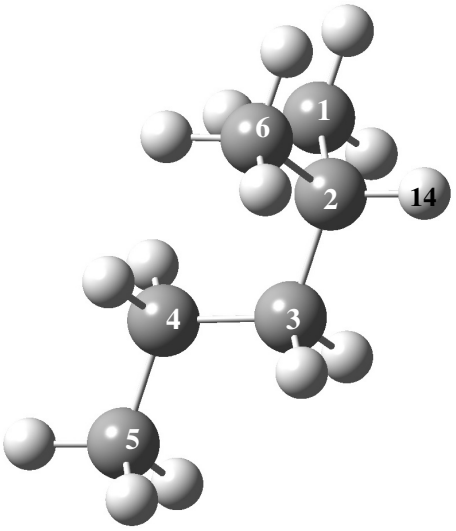


AA ($C_5$-$C_4$-$C_3$-$C_2$ anti, $C_4$-$C_3$-$C_2$-$H_{14}$ anti) (Observed)

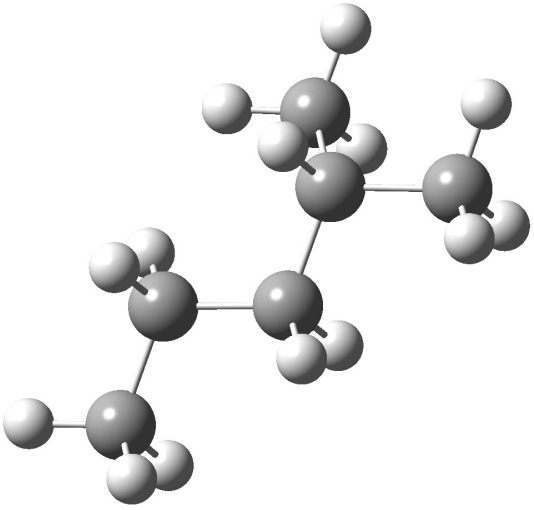

AG ($C_5$-$C_4$-$C_3$-$C_2$ anti, $C_4$-$C_3$-$C_2$-$H_{14}$ gauche) (Observed)

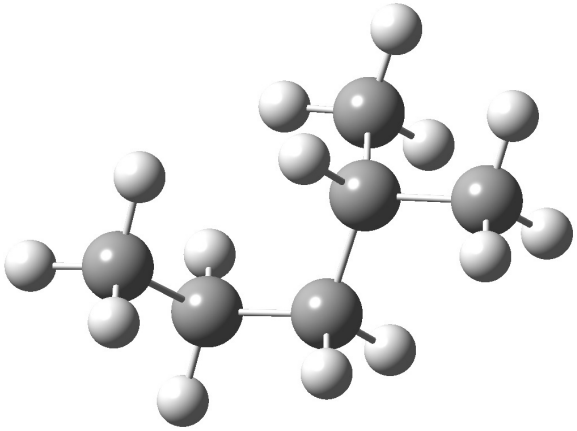

GG(cis) (Observed)

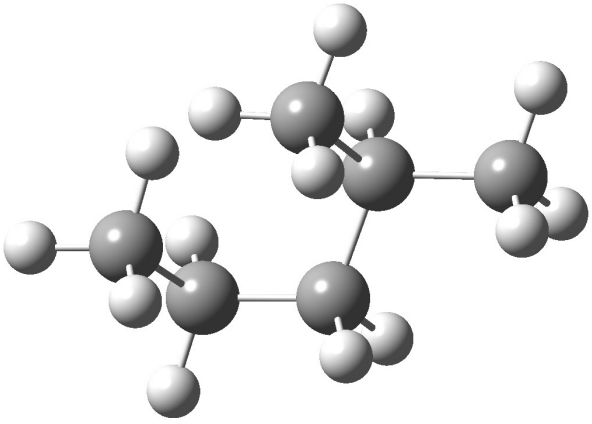

GG(trans) (Not Observed)

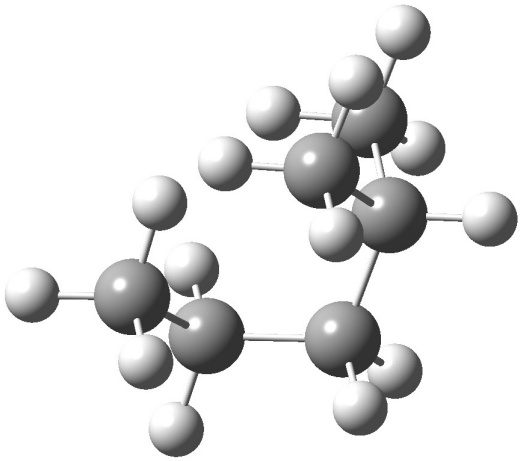

GA (Not Observed)

## Experimental

**MHept.** A sample of MHept was purchased from GFS Chemicals and used directly. The compound has a vapor pressure of ~8 torr at room temperature. A 7 L stainless steel tank was evacuated, ~1.5 g of sample distilled into it, and then filled to 4 atm with He to form a 0.3% sample mixture. Pulses of the mixture at 1 atm were introduced at 5 Hz into the pulsed jet-Fourier transform microwave spectrometer[5] of the Southern New England Microwave Consortium.[6] Five microwave pulses were recorded for each gas pulse and rotational transitions were observed between 8.9 and 19.4 GHz, although the complete spectral ranged was not measured. The rotational temperature of the expanded gas is estimated to be about 2 K. Measured transitions were observed as Doppler doublets and are estimated to be accurate to ~2 kHz.

**MPane.** Similarly, MPane was purchased from Aldrich Chemicals and used directly. A sample was distilled into a 7 L tank to a pressure of 0.04 atm and 4 atm He was added to give a 1% mixture. Rotational transitions were observed between 7.3 and 19.6 GHz, but the complete range was not scanned.

## Results

**MHept.** A molecular model for MHept was constructed from structures adjusted to approximately fit the rotational constants of 3-hexyne[1] and 4-methyl-1-pentyne.[4] This model structure was used to predict rotational constants and rotational transitions for the $C_1$ and $C_s$ conformers to MHept. The spectral fitting program jb95[7] was utilized to assign the rotational transitions. Rotational constants in jb95 were adjusted to match an intense pair of lines predicted to be the b-type transitions $2_{21}$-$1_{10}$ and $2_{20}$-$1_{11}$ between 14-15 GHz for the $C_1$ species. Several other transitions fell into place and a complete assignment was accomplished. A total of 39 lines were measured and assigned, of which 7 are a-types, 21 are b-types, and 11 are c-types. That the observed lines have all three types of selection rules confirms that the species has $C_1$ symmetry. The transitions were fit to an rmsd of 2.6 kHz using rotational constants and five quartic centrifugal distortion constants using Watson's S reduction in the $I^r$ representation.[8] The fitted spectroscopic constants are displayed in Table 1 and the assigned transitions are in Supplementary Table 1.

After the initial assignment of the $C_1$ conformer, only about 10 unassigned lines remained. They included a pair of intense lines around 17328/17329 MHz which were close to the predicted $3_{31}$-$2_{20}$/$3_{30}$-$2_{21}$ transitions of the $C_s$ conformer. The 10734/10792 MHz pair looked promising as the related $2_{21}$-$1_{10}$/$2_{20}$-$1_{11}$ predicted pair. This tentative four line assignment was correct and many more lines were predicted and measured for the $C_s$ species. A total of 53 lines were observed, of which 8 are a-type and 45 are b-type. The lack of c-type lines suggests that the species is of $C_s$ symmetry because it lacks a c-dipole due to an ab plane of symmetry. The transitions were fit to rotational constants, 5 quartic and 1 sextic centrifugal distortion constant to an rmsd of 3.4 kHz using Watson's S reduction in the $I^r$ representation.[8] The spectroscopic constants are listed in Table 1 and the assigned lines are given in Supplementary Table 1.

Table 1. Spectroscopic constants for 6-methyl-3-heptyne.

| | $C_S$ | $C_1$ |
|---|---|---|
| A/MHz | 3282.9197(6) | 4603.7990(7) |
| B/MHz | 942.43143(20) | 798.12154(13) |
| C/MHz | 886.33450(16) | 713.87656(11) |
| $P_{aa}$/uÅ$^2$ | 476.25 | 615.69 |
| $P_{bb}$/uÅ$^2$ | 93.49 | 92.25 |
| $P_{cc}$/uÅ$^2$ | 60.00 | 17.52 |
| $D_J$/kHz | 0.7372(12) | 0.2057(5) |
| $D_{JK}$/kHz | 9.776(24) | -1.611(9) |
| $D_K$/kHz | -5.383(17) | 24.93(14) |
| $d_1$/kHz | -0.1104(10) | -0.0289(3) |
| $d_2$/kHz | 0.1468(4) | -0.0061(4) |
| $H_{JK}$/kHz | -0.00102(24) | |
| Kappa | -0.9532 | -0.9567 |
| No. Lines | 53 | 39 |
| rmsd/kHz | 3.4 | 2.6 |

**MPane.** Lines observed in the 15-16 and 18-19 GHz ranges fit a-type R-branch transitions expected for the AG conformer. Fitting those lines predicted b- and c-type transitions, which were observed and measured. A number of unassigned lines near 19 GHz plus two strong lines near 11 GHz appeared to be a-type R-branch lines of the GG(cis) conformer. That assignment was successful and predicted b- and c-type lines were found and measured. Three weak lines observed at 13955, 14017, and 14393 MHz appeared to match the pattern of the expected $4_{04}$-$3_{03}$, $4_{23}$-$3_{22}$, and $4_{13}$-$3_{12}$ lines of the symmetric AA conformer. That three line fit proved to be correct as a host of other transitions were measured and assigned. Only a- and c-type lines were observed for the AA conformer, consistent with a plane of symmetry and thus no b-dipole. The assignments of the spectra of the three conformers are given in Supplementary Table 2 and the fitted spectroscopic constants are listed in Table 2.

Table 2. Spectroscopic constants for 2-methylpentane.

| Parameter | $C_s$ (AA) | $C_1$ (AG) | $C_1$ (GG) |
|---|---|---|---|
| A/MHz | 5820.1248(5) | 6615.4521(10) | 5501.9431(11) |
| B/MHz | 1848.9706(3) | 1713.06566(20) | 1980.37687(20) |
| C/MHz | 1656.7897(4) | 1473.09913(11) | 1789.41065(20) |
| $P_{aa}$/uÅ$^2$ | 245.77 | 280.85 | 222.88 |
| $P_{bb}$/uÅ$^2$ | 59.27 | 62.23 | 59.44 |
| $P_{cc}$/uÅ$^2$ | 27.56 | 14.17 | 32.31 |
| $D_J$/kHz | 0.219(5) | 0.1377(17) | 0.5437(18) |
| $D_{JK}$/kHz | 2.86(4) | 1.392(13) | 3.970(9) |
| $D_K$/kHz | | | -1.45(23) |
| $d_1$/kHz | -0.010(4) | -0.0252(5) | -0.0468(25) |
| $d_2$/kHz | | -0.0061(4) | -0.0258(11) |
| $H_k$/kHz | | -0.52(5) | |
| Kappa | -0.9077 | -0.9067 | -0.8971 |
| No. Lines | 17 | 35 | 24 |
| rmsd/kHz | 1.7 | 2.3 | 0.8 |

## Discussion

**MHept.** Two conformers corresponding to gauche ($C_1$) and anti ($C_s$) orientations of the isobutyl group in MHept were expected and that expectation was fulfilled. The determination of the relative orientation of the ethyl and isobutyl groups about the acetylene axis in each conformer remained to be answered.

An accurate molecular structure of MHept cannot be determined unambiguously from the experimental data alone. However, a reasonable model is obtained by fitting models simultaneously to the known spectroscopic constants of 3-hexyne, which models the ethyl end of MHept, and 4-methyl-1-pentyne, which models the isobutyl end. The ethyl and isobutyl groups of MHept are expected to interact very little, thus, good estimates of the variation of spectroscopic constants with torsion about the acetylene axis can be made by simply rotating the rigid models of the ethyl and isobutyl groups about that axis.

With the isobutyl group in the gauche conformation (overall $C_1$ symmetry), the second moments $P_{aa}$, $P_{bb}$, and $P_{cc}$ were calculated as functions of torsional angle and are displayed in Figure 3. For a rigid structure, $P_{aa} = \sum(m_i a_i^2)$ and is a measure of the extension of the molecule along the a-axis. $P_{bb}$ and $P_{cc}$ are defined similarly. The values of the experimentally determined second moments are indicated in Figure 3 by horizontal

lines. The intersections of the observed and calculated second moment values are circled. It is evident that the observed structure corresponds to a torsional angle of ~320-330°. Therefore, like in 3-heptyne,[2] the ethyl group eclipses the approximate center of electron density of the asymmetric isobutyl group. The structure is shown in perspective in Figure 4 and is consistent with the model that the dominant interaction determining the orientation of the groups about the acetylene axis is the weak dispersion attraction between the groups.

$P_{aa}$, $P_{bb}$, and $P_{cc}$ were also calculated as functions of torsional angle for the symmetric conformer of the isobutyl group. These are displayed in Figure 3. It is clear that the torsional angle is 0°, consistent with overall $C_s$ symmetry and the lack of observable c-type transitions. Furthermore, the sum of the appropriate second moment of 4-methyl-1-pentyne, 56.1 uÅ$^2$, with twice the contribution of a $CH_2$ group, 1.6 uÅ$^2$, to account for the second moment of the ethyl fragment, gives 59.3 uÅ$^2$, in good agreement with the experimental value of 60.0 uÅ$^2$ for MHept. As in the case with the asymmetric conformer, the structure of the symmetric conformer is consistent with the model that the dominant interaction is the dispersion attraction between the ethyl and isobutyl groups. The structure of the symmetric conformer is shown in Figure 4.

A range of *ab initio* calculations were performed at the HF and MP2 levels of theory using the *Gaussian 03* suite of programs[9] up to a basis set level of MP2/6-311+G(d,p). The calculations confirm the geometric models used above. The gauche and anti forms are calculated to differ in energy by 0.3 kcal/mol, marginally smaller than the commonly accepted value of 0.6 kcal/mol.[10] This is consistent with a modest C-H to π-stabilization in hydrocarbon chains containing C≡C bonds which have been observed in related species.[11] The equilibrium torsional angles and the torsional barrier about the acetylene axis were not determined because in 3-hexyne, a smaller compound than MHept, calculations with much larger basis sets were required to predict the barrier.[3] Total energies were corrected for zero-point energies and harmonic frequencies were found to be positive, consistent with stable minima. The lowest frequencies for MHept are very small, consistent with a tiny torsional barrier. Relative populations at 298 K were calculated and are expected to be retained in the rotationally cold gas pulse.[12] A summary of the calculated results is presented in Table 3.

Figure 3. The second moments $P_{aa}$, $P_{bb}$, and $P_{cc}$ as functions of rigid rotation of an isobutyl group vs. an ethyl group about the acetylene axis of 6-methyl-3-heptyne for the asymmetric isobutyl (upper) and symmetric isobutyl (lower). The straight lines represent the observed second moments and the intersections are marked by the circles.

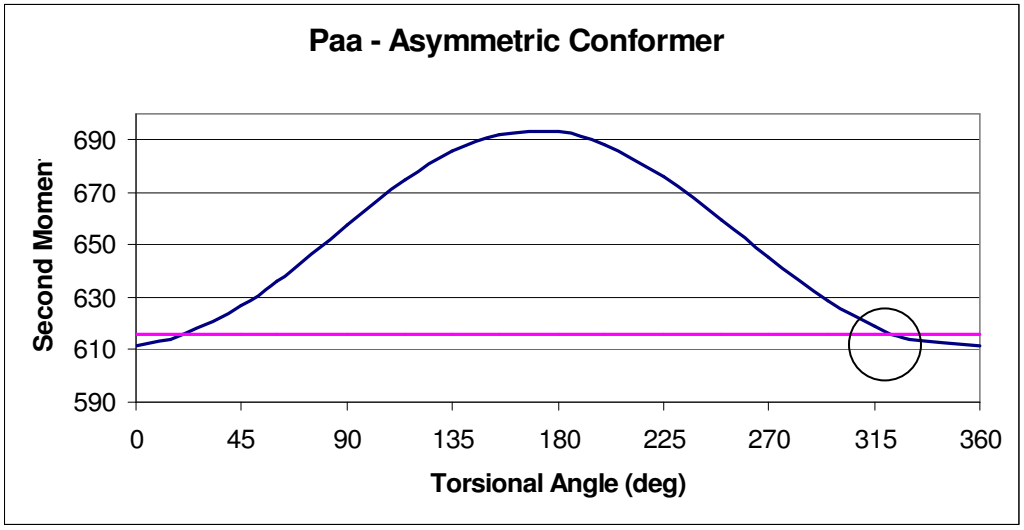


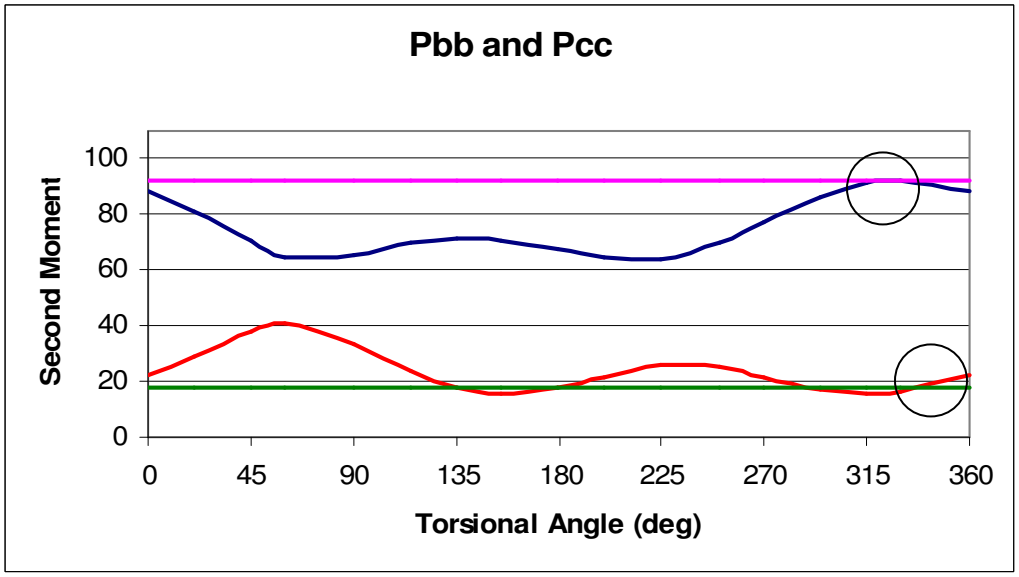

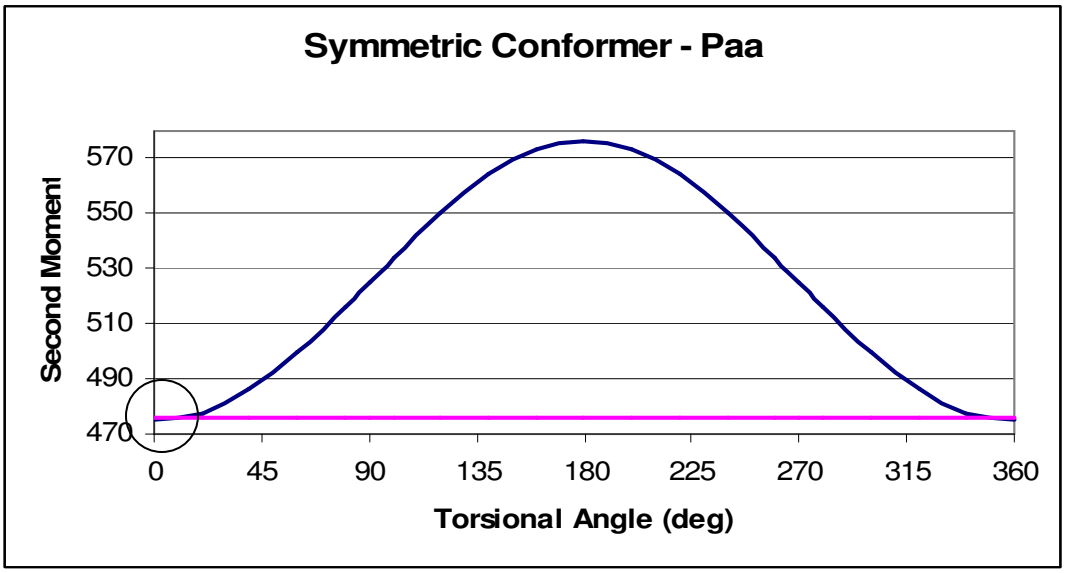
Symmetric Conformer - Paa
Second Moment
570
550
530
510
490
470
0
45
90
135
180
225
270
315
360
Torsional Angle (deg)

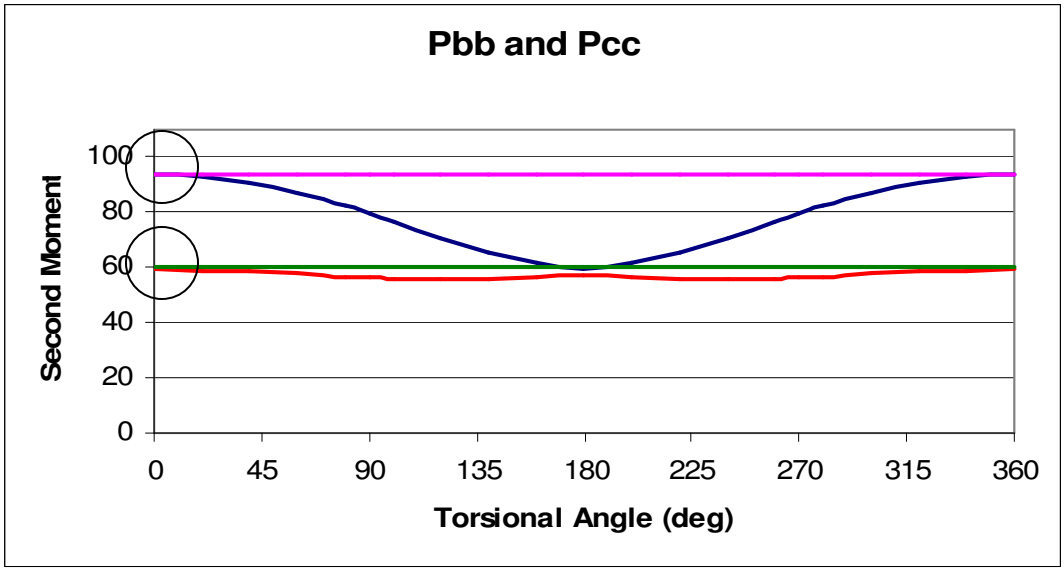
Pbb and Pcc
Second Moment
100
80
60
40
20
0
0
45
90
135
180
225
270
315
360
Torsional Angle (deg)

Figure 4. Perspective models of the observed conformers of 6-methyl-3-heptyne.

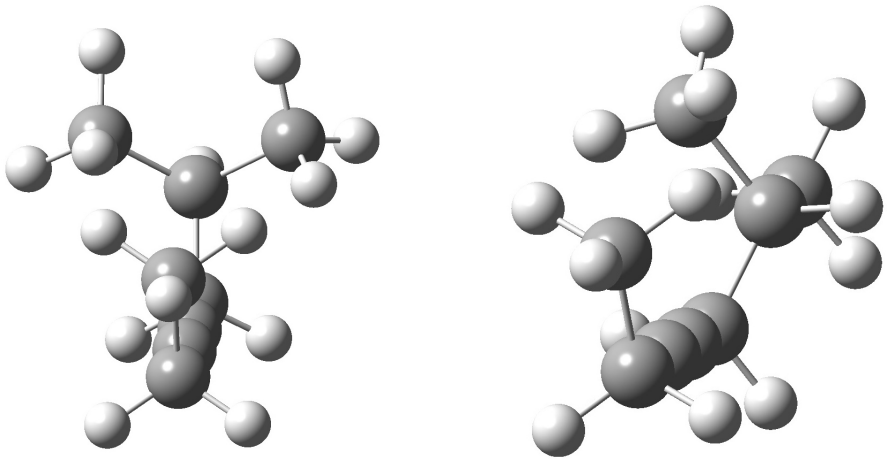

Eclipsed, $C_s$ Nearly eclipsed, $C_1$

**MPane.** The most intense rotational spectrum is observed from the AG species, which is predicted to be the most stable conformer. Identification of the observed conformers is unambiguous from a comparison of experimental and predicted spectroscopic constants. Quantum chemical calculations[9] of all five conformers of MPane were carried out at the MP2/6-311+G(d,p) level of theory. Rotational constants, relative energies, dipole moments, and relative abundances from the calculations for MPane are also listed in Table 3. Predicted and observed rotational constants are in excellent agreement and there is no ambiguity about the identity of the conformers displayed in Figure 2. The abundances predicted from the *ab initio* relative energies are consistent with the relative intensities of the transitions of the observed conformers. The higher relative energies of the GG(trans) and GA forms, 2-3 kcal/mol, demonstrate the significant steric repulsion of a 1-3 methyl-methyl interaction. Also, the higher minimum frequencies in MPane reflect the higher ethane-like torsional barrier compared to MHept.

The symmetric forms of MHept and MPane should have identical second moments out of the symmetry plane since both species have the same contribution from three pairs of methyl/methylene H-atoms and an isopropyl group, if the structures of the fragments are identical. $P_{cc}$ in MHept is 60.00 uÅ$^2$ and $P_{bb}$ of AA in MPane is 59.27 uÅ$^2$, in excellent agreement. The slightly larger value in MHept is consistent with its large amplitude out-of-plane torsion.

Table 3. Calculated and experimental properties of 6-methyl-3-heptyne and 2-methylpentane.

| Species/Method | $E_t/h$[a] | $E_{zp}/h$[b] | Rel. E/ kcal mol$^{-1}$ | A/MHz | B/MHz | C/MHz | Frequency /cm$^{-1}$ [c] | Dipole/D | Rel.[d] Abundance |
|---|---|---|---|---|---|---|---|---|---|
| *6-methyl-3-heptyne* | | | | | | | | | |
| $C_s$ symmetric form | | | | | | | | | |
| MP2/6-311+G(d,p) | -312.3064 | -312.1060 | 0.0 | 3264 | 949 | 887 | 8 | 0.25 | 47% |
| Experiment | | | | 3282.920 | 942.431 | 886.334 | | | |
| $C_1$ asymmetric form | | | | | | | | | |
| MP2/6-311+G(d,p) | -312.3059 | -312.1056 | 0.26 | 4630 | 799 | 712 | 12 | 0.30 | 53% |
| Experiment | | | | 4603.799 | 798.122 | 713.877 | | | |
| *2-methylpentane* | | | | | | | | | |
| AG, $C_1$ | | | | | | | | | |
| MP2/6-311+G(d,p) | -236.3563 | -236.1656 | 0.0 | 6651 | 1722 | 1477 | 78 | 0.13 | 58% |
| Experiment | | | | 6615.452 | 1713.066 | 1473.099 | | | |
| GG(cis), $C_1$ | | | | | | | | | |
| MP2/6-311+G(d,p) | -236.3562 | -236.1651 | 0.32 | 5531 | 2008 | 1811 | 85 | 0.09 | 34% |
| Experiment | | | | 5501.943 | 1980.377 | 1789.411 | | | |
| AA, $C_s$ | | | | | | | | | |
| MP2/6-311+G(d,p) | -236.3552 | -236.1643 | 0.85 | 5816 | 1822 | 1632 | 48 | 0.08 | 7% |
| Experiment | | | | 5820.125 | 1848.971 | 1656.790 | | | |
| GG(trans), $C_1$ | | | | | | | | | |
| MP2/6-311+G(d,p) | -236.3529 | -236.1619 | 2.31 | 5978 | 1980 | 1679 | 100 | 0.16 | 1.1% |
| GA, $C_1$ | | | | | | | | | |
| MP2/6-311+G(d,p) | -236.3517 | -236.1605 | 3.19 | 5080 | 2201 | 1878 | 78 | 0.10 | 0.3% |

[a] $E_t/h$ is total energy in hartree units.
[b] $E_{zp}/h$ is total energy corrected for zero point vibrations in hartree units.
[c] Lowest calculated harmonic frequency.
[d] Relative abundance at 298 K based on calculated energies and degeneracies of 2 for all conformers except $C_s$ (1).

## Summary

Two conformers of 6-methyl-3-heptyne have been identified and characterized from their microwave rotational spectra. The two conformers, of $C_1$ and $C_s$ symmetry, arise from the expected asymmetric and symmetric conformations of the isobutyl group. Unlike in saturated alkanes, the dominant interaction determining the orientation of the end groups about the acetylene axis is the weak dispersion attraction. This dispersion

attraction results in syn-eclipsed structures or nearly so. Quantum mechanical computations are consistent with those results.

The three lowest energy conformers of 2-methylpentane, which is 6-methyl-3-heptyne without the C≡C spacer, were also characterized by their rotational spectra. The conformations are the conventional staggered forms expected about C-C single bonds in saturated hydrocarbons due to the close proximity of the ethyl and isobutyl groups. Quantum mechanical computations confirm these results and show the energies of the remaining two possible conformers, which were not observed, are much higher due to 1,3-methyl-methyl repulsions. These two studies show the how the main interaction between alkyl groups depend on distance.

## References


[1] Bohn, R.K. *J. Phys Chem. A* **2004**, *108*, 6814.
[2] Churchill, G.B; Bohn, R.K. *J. Phys. Chem. A* **2007**, *111*, 3513.
[3] Churchill, G.B, Wiberg, K.B.; Bohn, R.K.; Michels, H.H. *Int. J. Quantum Chem.* **2006**, *106*, 3364.
[4] Churchill, G.B; Milot, R.L.; Bohn, R.K. *J. Mol. Struct*. **2007**, *836*, 86.
[5] Balle, T.J.; Flygare, W.H. *Rev. Sci. Instr.* **1981**, *52*, 33.
[6] Hight-Walker, A.R.; Lou, Q.; Bohn, R.K.; Novick, S.E. *J. Molec. Struct.* **1995**, *346*, 187.
[7] Plusquellic, D.F.; Suenram, R.D.; Mate, B.; Jensen, J.O.; Samuels, A.C. *J. Chem. Phys.* **2001**, *115*, 3057.
[8] Watson, J. K. G. *Vibrational Spectra and Structure*, Vol. 6 (J. R. Durig, Ed.), Elsevier, Amsterdam, pp 1-89, 1977.
[9] Gaussian 03, Revision B.05, M. J. Frisch, G. W. Trucks, H. B. Schlegel, G. E. Scuseria, M. A. Robb, J. R. Cheeseman, J. A. Montgomery, Jr., T. Vreven, K. N. Kudin, J. C. Burant, J. M. Millam, S. S. Iyengar, J. Tomasi, V. Barone, B. Mennucci, M. Cossi, G. Scalmani, N. Rega, G. A. Petersson, H. Nakatsuji, M. Hada, M. Ehara, K. Toyota, R. Fukuda, J. Hasegawa, M. Ishida, T. Nakajima, Y. Honda, O. Kitao, H. Nakai, M. Klene, X. Li, J. E. Knox, H. P. Hratchian, J. B. Cross, C. Adamo, J. Jaramillo, R. Gomperts, R. E. Stratmann, O. Yazyev, A. J. Austin, R. Cammi, C. Pomelli, J. W. Ochterski, P. Y. Ayala, K. Morokuma, G. A. Voth, P. Salvador, J. J. Dannenberg, V. G. Zakrzewski, S. Dapprich, A. D. Daniels, M. C. Strain, O. Farkas, D. K. Malick, A. D. Rabuck, K. Raghavachari, J. B. Foresman, J. V. Ortiz, Q. Cui, A. G. Baboul, S. Clifford, J. Cioslowski, B. B. Stefanov, G. Liu, A. Liashenko, P. Piskorz, I. Komaromi, R. L. Martin, D. J. Fox, T. Keith, M. A. Al-Laham, C. Y. Peng, A. Nanayakkara, M. Challacombe, P. M. W. Gill, B. Johnson, W. Chen, M. W. Wong, C. Gonzalez, and J. A. Pople, Gaussian, Inc., Pittsburgh PA, 2003.
[10] Bartell, L.S.; Kohl, D.A. *J. Chem. Phys*. **1963**, *39*, 3097.

[11] Utzat, K.; Bohn, R.K.; Michels, H.H. *J. Mol. Struct*. **2007**, *841*, 22.
[12] Ruoff, R.S.; Klots, T.D.; Emilsson, T.; Gutowsky, H.S. *J. Chem. Phys*. **1990**, *93*, 3142.

# Chapter 3. Conformational Studies of the Extended Butane Analogue 3,5-octadiyne

## Introduction

Saturated hydrocarbons are known to exhibit staggered structures with dihedral angles of $180^o$ or $\pm 60^o$ from the eclipsed position ($0^o$). The simplest case is ethane, which can exist in either a staggered or eclipsed conformation. The barrier to internal rotation was established in the 1930's to be about 3 kcal/mol through analysis of thermodynamic data,[1] with the staggered form being the favorable structure. Various experimental and computational studies on ethane and other compounds have verified the value of the rotational barrier.[2] The traditional explanation for the stability of the staggered form is that steric (exchange) repulsions[3] between the H atoms are minimized in the staggered state. This explanation has been vigorously debated in recent years. Weinhold and colleagues suggested that the stabilization of the staggered form was due to overlap of the C-H bonding orbitals with the trans vicinal C-H antibonding orbitals ($\sigma_{C\text{-}H} - \sigma^*_{C\text{-}H}$), termed hyperconjugation.[4] Pophristic and Goodman, using the natural bond orbital (NBO) methods established by Weinhold, showed that the exclusion of hyperconjugation made the eclipsed form of ethane lower in energy than the staggered form. The addition of hyperconjugative interactions in their calculations re-established the stability of the staggered conformer.[5] This result was questioned by numerous researchers. One study[6] divided the energy of ethane into three parts: Pauli (steric) repulsions, electrostatic interactions, and orbital interactions. Pauli repulsions were determined to dominate the rotational barrier in ethane, while electrostatic and orbital interactions (the hyperconjugative attractions) had little influence. A second study[7] utilized *ab initio* valence bond methods to show that steric repulsions contribute about two-thirds of the barrier height in ethane while hyperconjugation contributes the remaining one-third.

To experimentally test if hyperconjugation was the dominant interaction in determining the barrier to rotation in hydrocarbons, a microwave study of the butane analogue 3-hexyne ($CH_3CH_2C{\equiv}CCH_2CH_3$) was performed.[8] This compound can be thought of as two ethyl groups separated by a cylindrically symmetrical C≡C spacer. The addition of this spacer separates the ethyl end groups by about 4.5 Å, longer than the sums of the van der Waals radii of the separated H atoms (3.3 Å). At this distance, the steric interactions become weakly attractive. If the steric interactions for ethane are the dominant interactions, the structure of 3-hexyne should be syn-eclipsed due to the weak nonbonded attractions. Hyperconjugaton, on the other hand, relies on the symmetry of the bonding and antibonding orbitals. This symmetry is only achieved in a staggered structure for 3-hexyne, which would not be observable due to lack of a dipole moment. The microwave rotational spectrum of 3-hexyne was unambiguously assigned to the syn-eclipsed ($C_{2v}$) conformer, showing that the main interaction determining the orientation of the ethyl end groups about the acetylene axis is the weak nonbonded dispersion attraction. The butane analogue was chosen instead of the ethane analogue dimethylacetylene ($CH_3C{\equiv}CCH_3$) because the orientation of the methyl groups cannot be determined due to the three-fold symmetry of the methyl groups. Butane, however, does have similar potential function to ethane[9] and the barrier to rotation for both molecules should come from the same interactions.

A computational study of 3-hexyne[10] predicted the syn-eclipsed $C_{2v}$ structure to be the lowest energy form, in agreement with the experimental results. Large basis sets were required to accurately model the weak dispersion interactions. The staggered ($C_{2h}$) form was shown to be a transition state. The barrier to rotation in 3-hexyne is expected to be similar to that of dimethylacteylene, about 16 cal/mol.[11] The computations predict a barrier of about 20-30 cal/mol, much smaller than the ethane-like barrier of 3000 cal/mol.

In this study, analysis of the conformations of the more extended butane analogue 3,5-octadiyne ($CH_3CH_2C{\equiv}C\text{-}C{\equiv}CCH_2CH_3$) is performed. The addition of a second C≡C spacer increases the distance between the ethyl end groups by about 2.5 Å as compared to 3-hexyne (Figure 1). The dispersion attractions between the ethyl end groups are already very weak in 3-hexyne, so this added distance pushes the limit of this attractive force. An insight into the interaction in this compound is important for the characterization of

nonbonded attractive forces at long distances. This is of great significance for the understanding of dispersion interactions in large macromolecules such as proteins where these weak interactions are numerous and important.

Figure 1. The differences in distance between the ethyl end groups in 3-hexyne (left) and 3,5-octadiyne (right).

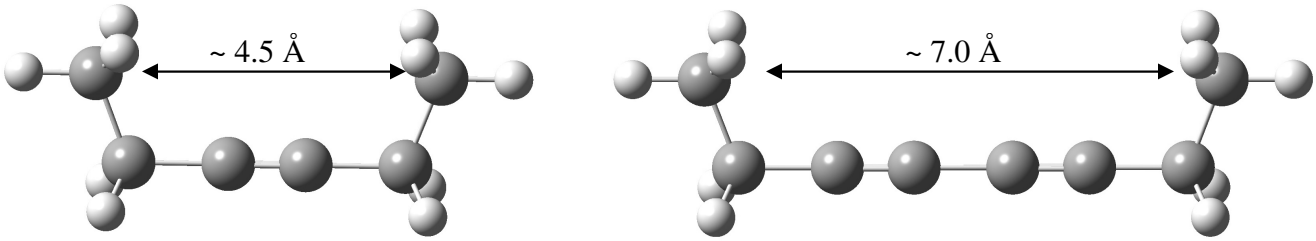


**Experimental**

A sample of 3,5-octadiyne was purchased from TCI America. GC-MS analysis showed the sample to be sufficiently pure. Several drops of the sample were placed in a copper U-tube in front of the nozzle of the pulsed-jet Fourier transform microwave spectrometer[12] of the Southern New England Microwave Consortium.[13] He was flowed over the 3,5-octadiyne sample, which has a vapor pressure of ~1 mm Hg at room temperature, at a pressure of 1-2 atm. Pulses of the mixed vapor were introduced into the spectrometer at 5 Hz and 5 microwave pulses were observed per gas pulse. The 8-16 GHz range was scanned, although the complete spectrum was not observed. The rotational temperature is predicted to be about 2 K.

A staggered ($C_{2h}$) 3,5-octadiyne structure does not have a dipole moment and would therefore not be observed with microwave spectroscopy. A $C_2$ structure has two degenerate orientations at $\pm\tau$ and the rotational transitions would be expected to show splittings due to the tunneling motion between the two orientations. No such tunneling splitting was observed. A syn-eclipsed ($C_{2v}$) structure has a b-dipole and expected to give relatively weak transitions. Modeling the $C_{2v}$ structure based on the observed $C_{2v}$ conformer of 3-hexyne predicts a simple rotational spectrum. A Q-branch is predicted to

be in the 8-9 GHz range and R-branch lines are predicted to span the 9-20 GHz range at ~1 GHz intervals. Extensive scanning for the Q-branch was unsuccessful. Turning to the R-branch ~5 lines were observed in the 14-15 GHz range, many more than expected. The line at 14013 MHz was much stronger than the others and was speculated to be the predicted $6_{16}$-$5_{05}$ transition. The proceeding $7_{17}$-$6_{06}$ line should have been ~ 1 GHz higher in frequency and a line was observed at 15094 MHz, a spacing of 1081 MHz. Scanning continued for the $8_{18}$-$7_{07}$ transition, which should have appeared around 16274 MHz. No transition was observed. Searching ~1080 MHz below the original 14014 line produced a third line at 12931 MHz. Six more lines were found at lower frequencies at spacings of ~1080 MHz. The lowest observed transition is at 6425 MHz. It is uncertain if the pattern continues at lower frequencies since this is past the limits of the spectrometer. The nine observed lines in the family are displayed in Table 1. Structures of the possible conformations of 3,5-octadiyne are shown in Figure 2.

Table 1. Observed lines and spacings for 3,5-octadiyne.

| Freq./MHz | Spacing/MHz | Intensity/mV |
|---|---|---|
| 6425.8897 | | 0.3 |
| 7511.1477 | 1085.26 | 0.9 |
| 8596.2265 | 1085.08 | 1.2 |
| 9680.9535 | 1084.73 | 1.4 |
| 10765.1734 | 1084.22 | 1.0 |
| 11848.7506 | 1083.58 | 3.2 |
| 12931.5622 | 1082.81 | 4.0 |
| 14013.5085 | 1081.95 | 6.0 |
| 15094.5045 | 1081.00 | 1.6 |

Figure 2. The possible conformations of 3,5-octadiyne.

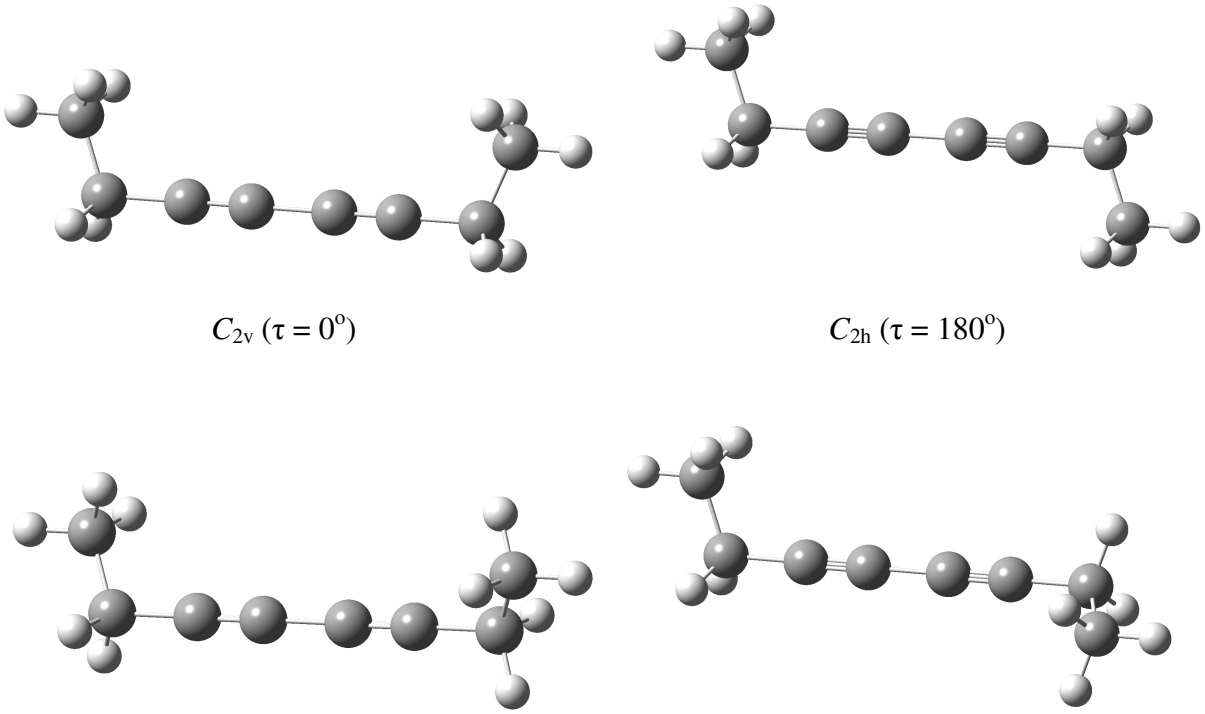

$C_{2v}$ ($\tau = 0^o$) $C_{2h}$ ($\tau = 180^o$)

$C_2$ ($0<\tau<90^o$) $C_2$ ($90<\tau<180^o$)

**Computations**

To determine relative stabilities and energies of the possible conformers of 3,5-octadiyne, *ab initio* quantum mechanical computations were performed at the Hartree-Fock (HF) and second-order Møller-Plesset (MP2) levels of theory with various basis sets. The computations were performed using the *Gaussian 03* suite of programs[14] implemented on a dual-processor Dell 530 workstation with the Linux operating system. Initial calculations were carried out with the Gaussian 6-31G* basis sets.[15,16] Calculations were then performed using the Dunning cc-pVDZ, cc-pVTZ, and cc-pVQZ correlation consistent valence basis sets.[17,18] Calculations carried out with these basis sets augmented by diffuse functions on both carbon and hydrogen were also performed.[17,19] In addition, calculations using Petersson's nZaP basis sets,[20] which are constructed in a similar manner to the Dunning set and designed to be used for extrapolation calculations, were carried out. Finally, calculations at the CCSD(T)/cc-

pVTZ level were performed and extrapolated to give an estimate of the energies at the CCSD(T)/aug-cc-pVQZ level. Optimized calculations were done with tight convergence criteria and harmonic vibrational frequencies were calculated for the HF/6-31G*, MP2/6-31G*, and MP2/cc-pVDZ optimized structures.

**Results and Discussion**

A computational study on 3-hexyne[10] predicted the lowest energy structure to be $C_2$ ($\tau$ ~±118°) using smaller basis sets. The eclipsed $C_{2v}$ structure was not predicted to be the lowest energy conformer until the very large aug-cc-pVQZ basis set was used, matching the experimental results.[8] Large basis sets are required to accurately model the weak dispersion interactions between the ethyl end groups. Using these large basis sets, the staggered $C_{2h}$ form was the highest in energy and frequency calculations showed it to be a transition state while the $C_{2v}$ form was a stable minimum. The energy difference between the $C_{2v}$ and $C_{2h}$ forms of 3-hexyne was found to be ~20-40 cal/mol. HF/6-31G* calculations on 3,5-octadiyne also predict the lowest energy form to be $C_2$. However, at the MP2/6-31G* and MP2/cc-pVDZ levels, this $C_2$ structure re-orients to the $C_{2h}$ and $C_{2v}$ forms, respectively. Calculations at the MP2/3ZaP levels did find a stable $C_2$ structure that is negligibly the lowest energy structure. Unlike in 3-hexyne, the $C_{2h}$ form of 3,5-octadiyne is consistently lower in energy than the $C_{2v}$ conformer at the HF and MP2 levels of theory. The best calculation, the extrapolated CCSD(T)/aug-cc-pVQZ calculation, predicts the $C_{2h}$ conformer to be less than 3 cal/mol lower in energy than the $C_{2v}$ conformer. The zero point vibrational energy (ZPVE) was taken into account for this extrapolation. The MP2/cc-pVDZ frequency calculations give ZPVE's of 0.152391 hartrees for the $C_{2h}$ conformer and 0.152398 hartrees for the $C_{2v}$ form. These values were corrected by the appropriate scale factor[21] of 0.9543. Frequency calculations also predict a tiny negative frequency for the $C_{2v}$ form, indicating that it might be a transition state. The $C_{2h}$ form has all positive frequencies, indicating a stable structure. The very small harmonic frequencies are consistent with an extremely flat potential surface. The barrier height between the $C_{2h}$ and $C_{2v}$ conformers is only ~1-10 cal/mol. The computational results are presented in Table 2.

Table 2. Relative energies and lowest harmonic frequencies for the possible conformers of 3,5-octadiyne.

| Level of Theory | $C_{2v}$ | $C_{2h}$ | $C_2$ | $C_2$ dihedral angle |
|---|---|---|---|---|
| HF/6-31G* | 3.0 (**$a_2$** = -2.47) | 1.8 (**$a_u$** = 0.25) | 0 | 98 |
| MP2/6-31G* | 37 (**$a_2$** = -66.7) | 0 (**$a_u$** = 1.89) | | |
| MP2/cc-pVDZ | 0 (**$a_2$** = -0.30) | 1.4 (**$a_u$** = 0.28) | | |
| MP2/cc-pVTZ | 2.2 | 0 | | |
| MP2/cc-pVTZ//(VDZ) | 1.6 | 0 | | |
| MP2/aug-cc-pVTZ//(VDZ) | 10.3 | 0 | | |
| MP2/cc-pVQZ//(VDZ) | 0.25 | 0 | | |
| MP2/aug-cc-pVQZ//(VDZ) | 1.8 | 0 | | |
| MP2/2ZaP | 4.7 | 0 | | |
| MP2/3ZaP | 5.6 | 0 | -0.45 | 134 |
| MP2/4ZAP//3ZaP | 2.7 | 0 | 32 | 134 |
| MP2/5ZAP//3ZaP | 1.4 | 0 | -0.34 | 134 |
| CCSD(T)/cc-pVTZ//(VDZ) | 0 | 1.8 | | |
| CCSD(T)/aug-cc-pVQZ[a,b] | 2.6 | 0 | | |

Energies in cal/mol.
Frequencies (**bold**) for the lowest torsional modes are in $cm^{-1}$.
[a] Estimated by the following equation: E(MP2/aug-cc-pVQZ//VDZ) + E(CCSD(T)/cc-pVTZ//VDZ) – E(MP2/cc-pVTZ//VDZ)
[b] Corrected for ZPVE.

To test the accuracies of the computations, the energy difference between the anti and gauche conformers of n-butane were calculated and compared to the established experimental difference of 660 ± 22 cal/mol.[22] The energy difference was calculated at the CCSD(T)/aug-cc-pVTZ level with the same extrapolation technique used with 3,5-octadiyne. Those results are presented in Table 3. The gauche conformer of butane was computed to be 686 cal/mol higher in energy than the anti form using this method, taking into account ZPVE's. This value is higher than the upper limit of the experimental value by about 4 cal/mol. It is evident, then, that the computed difference of 1-3 cal/mol at the highest levels of theory for 3,5-octadiyne is insignificant. This suggests that the $C_{2v}$ and $C_{2h}$ conformers of 3,5-ocatdiyne are essentially equal in energy and implies a zero rotational barrier.

Table 3. Comparison of the computed energy difference between the anti and gauche forms of butane to experimental.

| Level of Theory | Anti | Gauche |
|---|---|---|
| MP2/aug-cc-pVQZ//(VDZ)[a] | -158.1308 | -158.1299 |
| CCSD(T)/cc-pVTZ//(VDZ)[a] | -158.1531 | -158.1522 |
| MP2/cc-pVTZ//(VDZ)[a] | -158.0726 | -158.0717 |
| | | |
| CCSD(T)/aug-cc-pVQZ.[b] | -158.2113 | -158.2104 |
| ZPVE[a,c] | 0.1274 | 0.1275 |
| Relative Energy[d] | 0 | 686 |
| Experimental[d,e] | 0 | 660 ± 22 |

[a] Energies in hartrees.
[b] Estimated by the following equation: E(MP2/aug-cc-pVQZ//VDZ) + E(CCSD(T)/cc-pVTZ//VDZ) – E(MP2/cc-pVTZ//VDZ)
[c] Scaled by 0.9543, ref. 21.
[d] Energy in cal/mol.
[e] Ref. 22.

The fact that energy differences in the computational results are so small and that the dispersion interactions between the ethyl end groups were difficult to model in 3-hexyne allows for little confidence in the computational results for 3,5-octadiyne. The only way to confidently determine the lowest energy structure is through experiment. However, as described previously, microwave spectroscopic results have not been forthcoming. The observation of a spectrum means that the structure is not strictly $C_{2h}$, which has no dipole moment and would not give an observable spectrum. Tunneling splittings were not observed, so the structure cannot be strictly $C_2$. The observed transitions do not appear to be consistent with the simple pattern predicted for the $C_{2v}$ conformer. In order to fit the $K_p$ 1←0 family to the observed lines the $1_{11}$-$0_{00}$ transition must be at 6425 MHz, much lower that the predicted frequency of ~9000 MHz. This large shift downward in frequency results in a drastic decrease in the A constant, from ~8000 MHz to ~5000 MHz. It is also uncertain if the pattern continues below 6425 MHz. If it does, then the A constant will become even smaller. Fitting the $K_p$ 1←0 family to the observed transitions gives B = 544.2 MHz and C = 542.9 MHz, a nearly symmetric top, independent of where the family begins. The predicted B and C values for the $C_{2v}$ form are 562 and 534 MHz, not nearly as symmetric as the observed transitions. Furthermore, the addition of two quartic centrifugal distortion constants

changes the assignment from b-type lines to c-types. At around 90° there is an inversion of the rotational axis from b to c. Therefore, the observed transitions are unlikely to be from a $C_{2v}$ structure. The fitted spectroscopic constant from the $K_p$ 1←0 assignment are displayed in Table 4.

Table 4. Spectroscopic constants fitted for the assigned $K_p$ 1←0 c-type transitions.

| | |
|---|---|
| A/MHz | 5883.1757(4) |
| B/MHz | 542.7486(2) |
| C/MHz | 542.3174(2) |
| $D_J$/kHz | 9.38(3) |
| $d_1$/kHz | 0.730(5) |
| Std. Dev./kHz | 0.36 |

The original model for 3,5-octadiyne was rotated about 180° to see how the rotational constants change as a function of the torsional angle. The A constant increases from ~8000 MHz at 0° to ~13000 MHz at 180°. B and C are closest to a symmetric top between ~90°-105° and are least symmetric at 0° and 180°. It is possible that the ethyl end groups are freely rotating, in which case the end groups would become close to symmetric. The "average" position of a freely rotating structure would be at 90°, consistent with our B and C values. However, the discrepancy in the A constant is still puzzling. The predicted A value for a 90° structure is about 10000 MHz and it is expected that a freely rotating structure would give an A constant larger than that predicted for the $C_{2v}$ conformer. Perhaps the $K_p$ 1←0 assignment of the observed lines is incorrect. A second family of lines, $K_p$ 0←1, can also be fit to the observed transitions beginning with $15_{015}$-$14_{113}$. Notice that in order to fit this family of lines, the transitions must also be c-types and not b-types. This fit gives A = 10482 MHz, B = 548 MHz, and C = 547 MHz. The A value here is more consistent with free rotation and a ~90° structure. However, these lines are predicted to be extremely weak so this assignment is probably unlikely. More experiments are required to verify these possible assignments.

In any case, it is evident that the dispersion attractions between the ethyl end groups are too weak at this extended distance of about 7 Å. Dispersion interactions, although very weak, play significant roles in large systems such as proteins because they

are so numerous. The knowledge that dispersion interactions are observed at 4.5 Å but not at 7 Å provided important information for understanding and modeling the structures of such macromolecular systems.

## References


[1] Kemp, J.D.; Pitzer, K.S. J. Chem. Phys. **1936**, *4*, 749. Kemp, J.D.; Pitzer, K.S. *J. Am. Chem. Soc.* **1937**, *59*, 276. Pitzer, K.S. *Discuss. Faraday Soc*. **1951**, *10*, 66.
[2] Pitzer, R.M. *Acc. Chem. Res*. **1983**, *16*, 207. Wilson, E.B. Jr. *Adv. Chem. Phys*. **1959**, *2*, 367. Smith, L.G. *J. Chem. Phys*. **1949**, *17*, 139. Weiss, S.; Leroi, G.E. *J. Chem. Phys.* **1968**, *48*, 962. Hirota, E.; Saito, S.; Endo, Y. *J. Chem. Phys*. **1979**, *71*, 1183.
[3] Pauling, L.C. *The Nature of the Chemical Bond*, 3rd ed.; Cornell University Press: Ithaca, NY, 1960. Sovers, O.J.; Kern, C.W.; Pitzer, R.M.; Karplus, M. *J. Chem. Phys*. **1968**, *49*, 2592.
[4] Reed, A.E.; Weinhold, F. *Isr. J. Chem*. **1991**, *31*, 277. Weinhold, F. *Nature* **2001**, *411*, 539.
[5] Pophristic, V.; Goodman, L. *Nature* **2001**, *411*, 565.
[6] Bickelhaupt, F.M.; Baerends, E.J. *Angew. Chem. Int. Ed*. **2003**, *42*, 4188.
[7] Mo, Y.; Mu, W.; Song, L.; Lin, M.; Zhang, Q.; Gao, J. *Angew. Chem*. **2004**, *116*, 2020.
[8] Bohn, R.K. *J. Phys. Chem. A* **2004**, *108*, 6814.
[9] Compton, D.A.C.; Montero, S.; Murphy, W.F. *J. Phys. Chem*. **1980**, *84*, 3587. Heenan, R.K.; Bartell, L.S. *J. Chem. Phys*. **1983**, *78*, 1270.
[10] Churchill, G.B.; Wiberg, K.B.; Bohn, R.K., Michels, H.H. *Int. J. Quantum Chem*. **2007**, *106*, 3364.
[11] Nakagawa, J.; Imachi, M.; Hayashi, M. *J. Mol. Struct*. **1984**, *112*, 201.
[12] Balle, T.J.; Flygare, W.H. *Rev. Sci. Instr.* **1981**, *52*, 33.
[13] Hight-Walker, A.R.; Lou, Q.; Bohn, R.K.; Novick, S.E. *J. Molec. Struct.* **1995**, *346*, 187.
[14] Gaussian 03, Revision B.05, M. J. Frisch, G. W. Trucks, H. B. Schlegel, G. E. Scuseria, M. A. Robb, J. R. Cheeseman, J. A. Montgomery, Jr., T. Vreven, K. N. Kudin, J. C. Burant, J. M. Millam, S. S. Iyengar, J. Tomasi, V. Barone, B. Mennucci, M. Cossi, G. Scalmani, N. Rega, G. A. Petersson, H. Nakatsuji, M. Hada, M. Ehara, K. Toyota, R. Fukuda, J. Hasegawa, M. Ishida, T. Nakajima, Y. Honda, O. Kitao, H. Nakai, M. Klene, X. Li, J. E. Knox, H. P. Hratchian, J. B. Cross, C. Adamo, J. Jaramillo, R. Gomperts, R. E. Stratmann, O. Yazyev, A. J. Austin, R. Cammi, C. Pomelli, J. W. Ochterski, P. Y. Ayala, K. Morokuma, G. A. Voth, P. Salvador, J. J. Dannenberg, V. G. Zakrzewski, S. Dapprich, A. D. Daniels, M. C. Strain, O. Farkas, D. K. Malick, A. D. Rabuck, K. Raghavachari, J. B. Foresman, J. V. Ortiz, Q. Cui, A. G. Baboul, S. Clifford, J. Cioslowski, B. B. Stefanov, G. Liu, A. Liashenko, P. Piskorz, I. Komaromi, R. L. Martin, D. J. Fox, T. Keith, M. A. Al-Laham, C. Y. Peng, A. Nanayakkara, M. Challacombe, P. M. W. Gill, B. Johnson, W. Chen, M. W. Wong, C. Gonzalez, and J. A. Pople, Gaussian, Inc., Pittsburgh PA, 2003.
[15] McLean, A.D.; Chandler, G.S. *J. Chem. Phys*. **1980**, *72*, 5639.
[16] Krishnan, R.; Binkley, J.S.; Seeger, R.; Pople, J.A. *J. Chem. Phys*. **1980**, *72*, 650.

[17] Kendall, R.; Dunning, T.H. Jr.; Harrison, R.J. *J. Chem. Phys*. **1992**, *96*, 6796.
[18] Dunning, T.H. Jr. *J. Chem. Phys*. **1989**, *90*, 1007.
[19] Woon, D.E.; Duning, T.H. Jr. *J. Chem. Phys*. **1993**, *98*, 1358.
[20] Zhang, S.; Barnes, E.C.; Petersson, G.A. *J. Chem. Phys*. **2008**, *129*, 184116.
[21] Sinha, P.; Boesch, S.E.; Wilson, A.K. *J. Phys. Chem. A* **2004**, *108*, 9213.
[22] Balabin, R.M. *J. Phys. Chem. A* **2009**, *113*, 1012.

# Chapter 4. Helical $C_2$ Structures of Perfluoropentane and Perfluorohexane

## Introduction

The structure of the important industrial polymer polytetrafluoroethylene (PTFE, Teflon©) has been studied extensively by X-ray diffraction on single fibers and shown to be helical.[1] A helix can be characterized from either a helical perspective or a molecular prospective. X-ray crystallographers use the helical perspective,[2] where the helix is defined by the following three parameters: the distance from each atom to the helical axis (helical radius), ρ; the helical angle about the helical axis, θ; and the translation from one atom to the next about the helical axis (pitch), d. In the molecular perspective, the helix is described as follows: the C-C bond length, r; the CCC bond angle φ, and the CCCC dihedral angle, τ. A visual representation of the two perspectives is shown in Figure 1. The mathematical relationships for converting between the two perspectives are known and are displayed in Equations 1 and 2.[2,3]

Figure 1 – Helical (left) and molecular (right) perspectives for describing a helix. The dashed line represents the helical axis and the blue circles represent $CF_2$ groups.

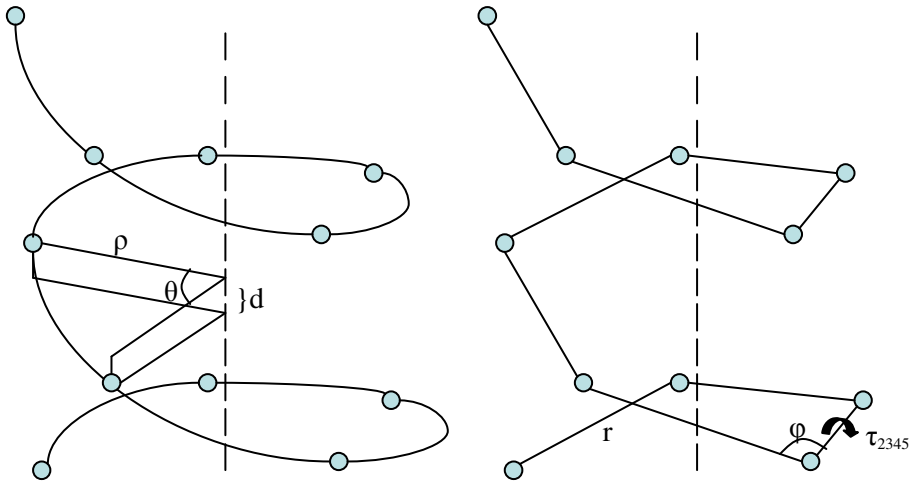


Equation 1. Helical parameters in terms of molecular parameters.

$$\cos\theta = \tfrac{1}{2}(-\cos\varphi + \cos\tau - \cos\varphi\cos\tau - 1)$$
$$d^2 = r^2(1 - \cos\tau)(1 - \cos\varphi)/(3 + \cos\varphi - \cos\tau + \cos\varphi\cos\tau)$$
$$\rho^2 = 2r^2(1 + \cos\varphi)/(3 + \cos\varphi - \cos\tau + \cos\varphi\cos\tau)^2$$

Equation 2. Molecular parameters in terms of helical parameters.

$$r^2 = d^2 + 4\rho^2\sin^2(\theta/2)$$
$$\cos(\varphi/2) = (1 - d^2/r^2)^{1/2}\sin(\theta/2)$$
$$\tan(\tau/2) = (d/r)\tan(\theta/2)$$

PTFE exists in several phases.[4] Below 19 $^oC$ (phase II) the chain twists 180$^o$ per 13 C atoms, a helical angle of 13.8$^o$. This is equal to ~163$^o$ CCCC dihedral angle, or ~17$^o$ away from trans. Between 19 $^oC$ and 30 $^oC$ (phase IV) the chain untwists slightly resulting in a 180$^o$ turn per 15 C atoms, or a helical angle of 12.0$^o$. Above 30 $^oC$ (phase I) further disorder enters the system but the helical angle remains unchanged. These phases are all disordered to various degrees so few molecular structure details are revealed, although the helicity is well characterized. Attempts to prepare single crystals of specific perfluorocarbon compounds without significant defects have not succeeded. The helicity

of PTFE is attributed to steric and dipole repulsions from F atoms of alternate carbons. A slight twist in the C chain alleviates these repulsions (Figures 2 and 3).

Experimental and computational studies on smaller perfluoroalkane oligomers have also revealed the lowest energy structures to be helical, beginning with perfluorobutane ($C_4F_{10}$).[5-15] Thin films of n-$C_{24}F_{50}$ have been studied by electron diffraction.[5] Unit cell information was determined but no molecular structural details. Early computational studies on $C_4F_{10}$ predicted three stable conformers: helical (trans), gauche, and ortho ($\tau \sim 90^o$).[6-7] Nitrogen matrix-isolate IR spectra of all three forms were assigned, with only small amounts of the ortho form observed.[8] Only the gauche form was observed in a microwave study with the dihedral angle determined to be $54.9^o \pm 2.4^o$.[16] Apparently, the helical form has too small a dipole moment to be observable and the ortho form relaxes to the lower energy gauche form.[17] The CCCC dihedral angle of $C_4F_{10}$ has not been determined experimentally and computations predict a twist of ~$14^o$ from trans.[6-13] The microwave spectrum of perfluoropropane ($C_3F_8$) has recently been assigned and the structure determined to be non-helical.[15] It appears that the steric and dipole repulsions are not sufficient in the three C chain to cause a twist in the structure. The complete $C_3F_8$ experiment and analysis is presented in Chapter 5.

Most of the computational studies have aimed to model PTFE and to computational reproduce the structural details of PTFE through force fields,[11,12] density functional theory,[10,14] and other methods.[7] To complement the computational studies, the structures of the lowest energy helical conformers of perfluoropentane ($C_5F_{12}$) and perfluorohexane ($C_6F_{14}$) were experimentally determined, in particular the value of the CCCC dihedral angle(s). The single CCCC dihedral angle in $C_5F_{12}$ is predicted to be ~16-17$^o$ from trans and the two CCCC dihedral angles in $C_6F_{14}$ are calculated to be ~16-18$^o$ from trans by various computational methods.[7,10-14] The microwave spectra of $C_5F_{12}$, its three $^{13}C$ isotopomers, and $C_6F_{14}$ have been observed and assigned and the molecular geometry analyzed.

Figure 2. Top view of perfluoropentane (left) and perfluorohexane (right) along the b-axis.

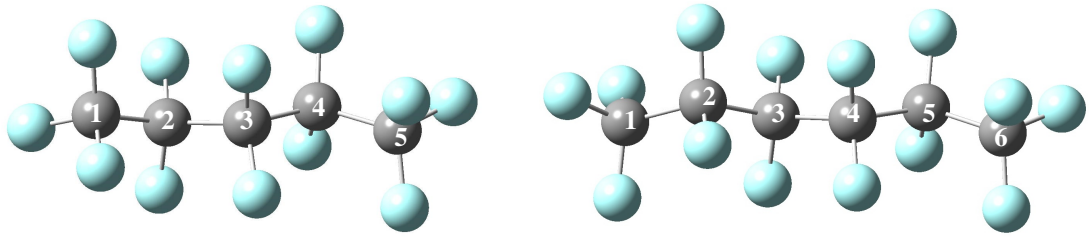


Figure 3. The staggered structure of n-pentane, $C_5H_{12}$, (far left) with dihedral angles of 180°, the helical structure of $C_5F_{12}$, (left-center), the staggered structure of n-hexane (right-center), and the helical structure of $C_6F_{14}$ (far right).

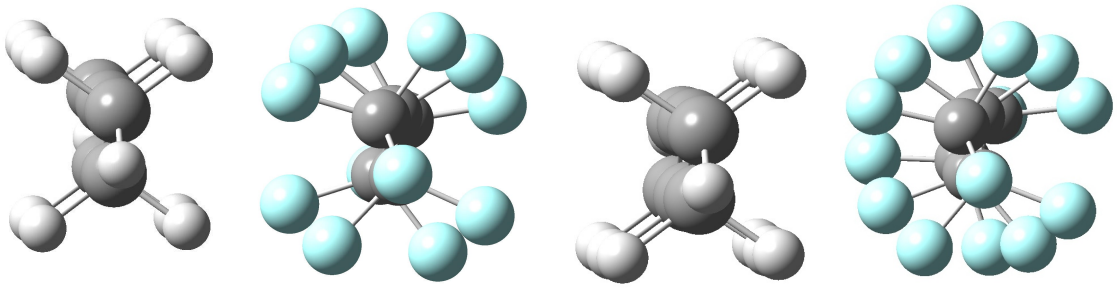

## Experimental

**$C_5F_{12}$.** $C_5F_{12}$ was purchased from Synquest Laboratories and used directly. Vapor of the sample was transferred to a 7 L stainless steel tank to a pressure of 0.09 atm. 4.5 atm He was added to produce a 2% sample mixture. The mixture flowed at 1.5 atm into the nozzle of the pulsed-jet Fourier transform microwave spectrometer[18] of the Southern New England Microwave Consortium.[19] Gas pulses were admitted at 5 Hz and five microwave pulses were observed per gas pulse. Transitions were observed in the 9-18 GHz range, although the complete spectrum was not observed. Transitions were observed as Doppler doublets with uncertainties estimated to be about 2 kHz. The rotational temperature of the expanded gas is estimated to be about 5 K.

**$C_6F_{14}$.** $C_6F_{14}$ was purchased from Synquest Laboratories and studied directly. Vapor of the sample was transferred to a 7 L stainless steel tank to a pressure of 0.04 atm and 6.5

atm He was added to produce a 0.6% mixture. Pulses of the sample mixture at 1.75 atm was admitted at 5 Hz into the pulsed-jet Fourier transform microwave spectrometer[18] of the Southern New England Microwave Consortium.[19] Five microwave pulses were observed per gas pulse. Rotational transitions were measured between 6-11 GHz, although the entire spectrum was not observed. Transitions were observed as Doppler doublets with estimated uncertainties of about 2 kHz and the rotational temperature of the expanded gas is estimated to be about 5 K.

## Results

**$C_5F_{12}$ Parent Isotopomer.** A b-type Q-branch with a band head near 11584 MHz was first observed in an automatic overnight scan. For a nearly prolate rotor with b-type transitions, Q-branches should be observed at spacings of 2(A – C). Another Q-branch was measured around 10220 MHz so that A – C is ~680 MHz. The 10220 MHz branch corresponds to $\Delta K_p$ of 8←7 and the 11584 MHz branch corresponds to $\Delta K_p$ of 9←8. The Q-branch lines are all doubly degenerate, meaning B and C are not distinguishable. Lower $K_p$ non-degenerate R-branch transitions were needed in order to distinguish B and C. The slightly separated (0.3 MHz) $9_{46}$-$8_{35}$/$9_{45}$-$8_{36}$ transitions were observed around 10335 MHz. This assignment was made and new lines were predicted and measured, refining the assignment. Rotational quantum numbers were observed up to J = 40 and $K_p$ = 9. The transitions were fit to rotational constants and three quartic centrifugal distortion constants using Watson's S reduction in the $I^r$ representation.[20] The complete list of assigned transitions is given in Supplementary Table 3. Spectroscopic constants are displayed in Table 1. The S/N ratio for many of the transitions was >100 allowing for the opportunity to measure $^{13}C$ isotopomers in natural abundance.

**$C_5F_{12}$ $^{13}C$ Isotopomers.** The initial parent model was adjusted to fit the observed rotational constants by simultaneously fitting the following 3 parameters: C-C bond length, CCC bond angle, and the CCCC dihedral angle. The rotational constants for the three possible $^{13}C$ isotopomers were predicted from this model and the Pickett suite of programs[21] was used to predict the most intense transitions. Since the natural abundance of $^{13}C$ is about 1%, the intensities of $^{13}C$ transitions are about 0.01 that of the parent

species. Assuming $C_2$ symmetry, the $^{13}C_1$ and $^{13}C_2$ positions in $C_5F_{12}$ are doubly degenerate allowing intensities of about 2% of that of the parent. Since $C_5F_{12}$ is nearly a symmetric top, there are many pairs of degenerate high $K_p$ transitions. This additional degeneracy allows for relatively intense lines for the $^{13}C_1$ and $^{13}C_2$ isotopomers. The observed intensities for the $^{13}C_1$ and $^{13}C_2$ isotopomers are twice that of the $^{13}C_3$ species, consistent with $C_2$ symmetry. Several of the degenerate transitions were observed for each $^{13}C$ isotopomer. The slightly split (<1 MHz) $10_{46}$-$9_{37}$/$10_{47}$-$9_{36}$ pair was observed for all three $^{13}C$ isotopomers and the inclusion of these lines into the fits distinguished B and C. Other non-degenerate transitions were predicted from the improved fits and measured. The centrifugal distortion constants were held fixed at the values determined for the parent. The fitted spectroscopic constants are shown in Table 1 and the assigned transitions are listed in Supplementary Table 4.

It is curious that B is different for the parent species and the $^{13}C_3$ isotopomer. $^{13}C_3$ lies directly on the b-axis and, thus, has no contribution to the moment of inertia about the b-axis. Therefore, for a rigid molecule, B for the parent and the $^{13}C_3$ isotopomer should be identical. Likewise, the second moments along the a and c-axes, $P_{aa}$ and $P_{cc}$, should also be identical for the parent and $^{13}C_3$ species. $P_{aa}$ and $P_{cc}$ for the $^{13}C_3$ species are actually smaller than those of the parent. The largest difference is in $P_{aa}$, which is 0.08 u$Å^2$ smaller for $^{13}C_3$ than for the parent. For a rigid molecule, the location of an atom is the same for all its isotopes. $C_5F_{12}$ appears to be a very rigid molecule from the evidence of its small centrifugal distortion constants. Substitution of $^{13}C$ for $^{12}C$ only changes the molar mass by one part in 288. It is not clear why the zero point vibrations cause the variations in B and the second moments of the $^{13}C_3$ species.

**$C_6F_{14}$.** Three observed transitions at 7624.38 MHz, 8024.94 MHz, and 8425.50 MHz were tentatively assigned to the $5_{50}$-$4_{40}$/$5_{51}$-$4_{41}$, $6_{51}$-$5_{41}$/$6_{52}$-$5_{42}$, and $7_{52}$-$6_{42}$/$7_{53}$-$6_{43}$ degenerate pairs, respectively. This tentative assignment predicted the $8_{53}$-$7_{43}$/$8_{54}$-$7_{44}$ degenerate pair to be around 8826 MHz. A line was observed at 8826.05 MHz, proving the assignment correct, and several more of these degenerate pairs were measured. Since the transitions are doubly degenerate, B and C are not distinguishable. A host of non-degenerate lines were predicted from the new assignment and were measured to

distinguish B and C. The transitions were fit using rotational constants and one quartic centrifugal distortion constant using Watson's S reduction[20] in the $I^r$ representation to an rmsd of 1.8 kHz. The use of only one centrifugal distortion constant that is quite small indicates that $C_6F_{14}$ is very rigid. The observed spectroscopic constants are displayed in Table 1 and the 46 assigned transitions are listed in Supplementary Table 5.

**Computations.** Quantum chemical computations were performed using the *Gaussian 03* program.[22] The computed second moments $P_{bb}$ and $P_{cc}$ of $C_5F_{12}$ for optimized models at various levels of theory are in excellent agreement with those observed. Each of the computed $P_{aa}$ second moments are lower than the observed 1379.87 uÅ$^2$, indicating that the computed models are too short along the a-axis. The MP2/VTZ model is our best computed structure for $C_5F_{12}$. The PBE0 functional, by suggestion of reference 14, is shown to give values that agree well with those observed. The PBE0/VTZ model of $C_5F_{12}$ was not significantly different from the MP2/VTZ model and the calculation cost was much less than that at the MP2 level. For this reason, $C_6F_{14}$ calculations were performed at the PBE0/VTZ level and not at the MP2 level. The PBE0/VTZ model of $C_6F_{14}$ is also in excellent agreement with the observed spectroscopic constants. Comparison of the observed and computed spectroscopic constants of $C_5F_{12}$ and $C_6F_{14}$ is given in Table 2.

Table 1. Spectroscopic constants for $C_5F_{12}$, its three $^{13}C$ isotopomers, and $C_6F_{14}$.

| | $C_5F_{12}$ Parent | $^{13}C_1$ | $^{13}C_2$ | $^{13}C_3$ | $C_6F_{14}$ |
|---|---|---|---|---|---|
| A/MHz | 990.6394(3) | 990.5179(1) | 990.0905(2) | 990.4427(2) | 824.9001(9) |
| B/MHz | 314.0002(1) | 312.6860(2) | 313.6872(2) | 314.0167(3) | 202.2195(8) |
| C/MHz | 304.3703(1) | 303.1237(1) | 304.0333(1) | 304.3654(2) | 198.3355(10) |
| $D_J$/kHz | 0.00365(13) | [0.00365] [a] | [0.00365] [a] | [0.00365] [a] | 0.00165(13) |
| $D_{JK}$/kHz | 0.00220(19) | [0.00220] [a] | [0.00220] [a] | [0.00220] [a] | |
| $D_K$/kHz | 0.0094(3) | [0.0094] [a] | [0.0094] [a] | [0.0094] [a] | |
| $P_{aa}$/uÅ$^2$ | 1379.8703 | 1386.6356 | 1381.4523 | 1379.7909 | 2217.3039 |
| $P_{bb}$/uÅ$^2$ | 280.5382 | 280.6015 | 280.7969 | 280.6445 | 330.7979 |
| $P_{cc}$/uÅ$^2$ | 229.6162 | 229.6155 | 229.6403 | 229.6112 | 281.8569 |
| Kappa | -0.971936 | -0.972178 | -0.971857 | -0.971865 | -0.9876022 |
| No. Lines | 201 | 44 | 22 | 23 | 46 |
| Std. Dev./kHz | 1.3 | 1.8 | 1.0 | 2.0 | 1.8 |

[a] Centrifugal distortion constants for the $^{13}C$ isotopomers were held fixed at the parent values.

Table 2. Comparison of observed spectroscopic constants to computed values.

| | $C_5F_{12}$ | | | $C_6F_{14}$ | |
|---|---|---|---|---|---|
| | Obs'd | MP2/VTZ | PBE0/VTZ | Obs'd | PBE0/VTZ |
| A/MHz | 990.6394 | 991.9 | 994.7 | 824.9001 | 828.6 |
| B/MHz | 314.0002 | 316.3 | 314.3 | 202.2195 | 202.3 |
| C/MHz | 304.3703 | 306.7 | 304.6 | 198.3355 | 198.4 |
| $P_{aa}$/uÅ$^2$ | 1379.870 | 1368.2 | 1379.7 | 2217.304 | 2217.5 |
| $P_{bb}$/uÅ$^2$ | 280.538 | 279.8 | 279.7 | 330.798 | 329.7 |
| $P_{cc}$/uÅ$^2$ | 229.616 | 229.8 | 228.4 | 281.857 | 280.2 |

## Discussion

**$C_5F_{12}$.** The microwave results do not provide sufficient information to unambiguously define the magnitude of the CCCC dihedral angle from exactly trans. The experimental data provide twelve total moments of inertia, 3 from the parent species and 3 from each of the three $^{13}C$ singly-substituted isotopomers. Those of the $^{13}C$ isotopomers are moments of species which differ only by one mass unit out of 288, so these values are closely correlated. There are a variety of constraints which can be placed upon the analysis to evaluate the dihedral angle. Assuming overall $C_2$ symmetry, there are 23 structural parameters required to specify the molecular geometry, many more than independent data points. As a first model, the following assumptions were made: the terminal $CF_3$ groups have local $C_{3v}$ symmetry and the internal $CF_2$ groups have local $C_{2v}$ symmetry. Initial values for bond lengths and bond angles were taken from our MP2/VTZ calculations, averaged according to the $CF_3/CF_2$ symmetry constraints, and differences among the various bond lengths and bond angles were held constant at the *ab initio* values. Various $r_0$ calculations were performed simultaneously fitting the 12 observed second moments (Table 3). Between 5 and 9 structural parameters were allowed to vary, giving a range of $16^o \pm 3^o$ for the dihedral angle. The first $r_0$ structure varied the following 5 parameters: C-C bond lengths together, C-F bond lengths together, CCC bond angles together, FCC bond angles together, and the CCCC dihedral angle. A 6 parameter fit varied the C-C bond lengths together, the $C_1C_2C_3$ and $C_2C_3C_4$ bond angles independently, the C-F bond lengths together, the FCC bond angles together, and the CCCC dihedral angle. An alternative 6 parameter fit allowed the $C_1$-$C_2$ and $C_2$-$C_3$ bond

lengths to vary independently while restricting the two CCC bond angles to vary by the same amount. A 7 parameter fit allowed the two C-C bond lengths and the two CCC bond angles to each vary independently. In the 9 parameter fit the three FCC bond angles were allowed to vary independently along with the two C-C bond lengths, the two CCC bond angles, the C-F bond lengths together, and the CCCC dihedral angle. The standard deviations of the second moments for each fit were well below the 0.08 u$Å^2$ difference seen in the experimental results.

There are several inconsistencies in the output structural values. The *ab initio* model predicts the $C_1$-$C_2$ and $C_2$-$C_3$ bond lengths to be nearly equal. When the two bond lengths were allowed to vary independently, the $C_1$-$C_2$ bond length became about 0.02 Å longer than the $C_2$-$C_3$ bond length. Additionally, bond lengths for several of the fits increased to around 1.57 Å, unusually long for a C-C bond length. It is evident, then, that the structural values and the dihedral angle are quite sensitive to the constraints placed on the model. This inconsistency is thought to derive in part from the assumption of local symmetry for the $CF_3$ and $CF_2$ groups.

A completely independent method to determine the dihedral angle is Kraitchman's method[23] which determines the coordinates of an isotopically substituted atom from the differences between the parent and isotopomer's moments. Since all the C atoms in the chain have been substituted, the method gives C-C bond lengths, CCC bond angles, and the CCCC dihedral angle. Those are also displayed in Table 3. Since the second moments $P_{aa}$ and $P_{cc}$ for the $^{13}C_3$ species are smaller than those of the parent when they should be identical, the a and c coordinates for $^{13}C_3$ are imaginary in the Kraitchman approach. Furthermore, the two C-C bond lengths in the determined structure differ by 0.03Å, which is unreasonable. Kraitchman's method appears to be an unreliable approach in the case of $C_5F_{12}$.

Table 3. Output structural parameters of $C_5F_{12}$ for various $r_0$ calculations and Kraitchman analysis. The standard deviations are in the second moments.

| | MP2/VTZ | 5 par. | 6 par. | 6 par. | 7 par. | 9 par. | Kraitchman |
|---|---|---|---|---|---|---|---|
| $C_1$-$C_2$ | 1.549 | 1.572 | 1.558 | 1.579 | 1.566 | 1.554 | 1.552 |
| $C_2$-$C_3$ | 1.551 | 1.574 | 1.560 | 1.552 | 1.550 | 1.532 | 1.517 |
| $\angle C_1C_2C_3$ | 113.9 | 112.2 | 113.8 | 112.9 | 113.8 | 115.6 | 115.9 |
| $\angle C_2C_3C_4$ | 113.0 | 111.3 | 110.9 | 112.0 | 111.4 | 113.9 | 113.2 |
| $C_1C_2C_3C_4$ | 16.8 | 19.2 | 13.7 | 17.2 | 13.9 | 16.4 | 13.3 |
| Std. Dev./ uÅ$^2$ | 9.85 | 0.025 | 0.025 | 0.025 | 0.026 | 0.033 | |

A third approach, assuming only overall $C_2$ symmetry, was then suggested to determine the dihedral angle. The principal coordinates from the *ab initio* computations were scaled by the square root of the ratio of the observed second moments to the computed second moments. This scaling approach shifts the coordinates of each atom giving a new structure which reproduces the observed second moments for the parent. The scaling ratios using the MP2/VTZ model are 1.0043 for the a-coordinate, 1.0014 for the b-coordinate, and 0.9997 for the c-coordinate. Since the scaling ratios are nearly equal to 1 the changes in the structural parameters are minor. The most noticeable change from the *ab initio* structure to the scaled structure is the increased length of each C-C bond by 0.005Å. The CCC bond angles each increased by 0.2$^o$ and the dihedral angle changed insignificantly (Table 4). These slight increases in the bond lengths and bond angles are consistent with a small increase in $P_{aa}$, which is underestimated by the *ab initio* models. The $C_1$, $C_2$, and $C_3$ positions in the scaled parent structure were then each substituted by mass 13, resulting in accurate predictions of the second moments for the three $^{13}C$ isotopomers (Table 5). That the second moments for the three isotopomers are in close agreement with the observed values indicates that the scaled MP2/VTZ structure is an excellent model. The scaling was performed on models calculated at various levels of theory and resulted in a narrow range for the dihedral angle of 17$^o$ ± 1$^o$ and overall more consistency in the structure compared to the $r_0$ structures (Table 6). The standard deviations in the second moments for each scaling are near or below 0.08 uÅ$^2$, with the best results from the scaling of the MP2/VTZ model. This scaled structure gives bond lengths of 1.554Å and 1.556Å for $C_1$-$C_2$ and $C_2$-$C_3$, respectively; 114.1$^o$ and 113.2$^o$ for $C_1C_2C_3$ and $C_2C_3C_4$, respectively; and a dihedral angle of 16.8$^o$. Converting to helical

parameters using Equations 1 and 2, averaging bond lengths and bond angles, gives a helical angle of 14.1°, a helical radius of 0.431Å, and a pitch of 1.297Å. These values are in good agreement with the 13.8° helical angle, 0.42Å helical radius, and 1.292Å pitch determined for the low temperature (phase II) form of PTFE.[3]

Table 4. Comparison of selected scaled and computed structural parameters for $C_5F_{12}$ and $C_6F_{14}$.

| | $C_5F_{12}$ | | | | $C_6F_{14}$ | |
|---|---|---|---|---|---|---|
| | Scaled MP2/VTZ | MP2/VTZ | Scaled PBE0/VTZ | PBE0/VTZ | Scaled PBE0/VTZ | PBE0/VTZ |
| $C_1$-$C_2$ | 1.554 | 1.549 | 1.556 | 1.555 | 1.556 | 1.555 |
| $C_2$-$C_3$ | 1.556 | 1.551 | 1.558 | 1.557 | 1.559 | 1.558 |
| $C_3$-$C_4$ | | | | | 1.561 | 1.561 |
| $\angle C_1C_2C_3$ | 114.1 | 113.9 | 113.9 | 114.0 | 113.9 | 114.0 |
| $\angle C_2C_3C_4$ | 113.2 | 113.0 | 113.1 | 113.2 | 112.9 | 113.0 |
| $C_1C_2C_3C_4$ | 16.8 | 16.8 | 16.7 | 16.6 | 16.7 | 16.7 |
| $C_2C_3C_4C_5$ | | | | | 18.0 | 18.0 |

Table 5. Comparison of observed and scaled second moments of $C_5F_{12}$.

| | $P_{aa}$ | | | $P_{bb}$ | | | $P_{cc}$ | | |
|---|---|---|---|---|---|---|---|---|---|
| | Obs'd | Scaled | MP2/VTZ | Obs'd | Scaled | MP2/VTZ | Obs'd | Scaled | MP2/VTZ |
| Parent | 1379.87 | 1379.88 | 1368.16 | 280.54 | 280.54 | 279.76 | 229.62 | 229.62 | 229.76 |
| $^{13}C_1$ | 1386.64 | 1386.68 | | 280.60 | 280.61 | | 229.62 | 229.62 | |
| $^{13}C_2$ | 1381.45 | 1381.53 | | 280.80 | 280.80 | | 229.64 | 229.65 | |
| $^{13}C_3$ | 1379.79 | 1379.88 | | 280.65 | 280.65 | | 229.61 | 229.62 | |

Table 6. Scaled $C_5F_{12}$ structures from models calculated at various levels of theory. The standard deviations are in the second moments.

| | MP2/ 6-31G* | PBE0/ 6-31G* | MP2/ 6-311+G* | PBE0/ 6-311+G* | MP2/ VDZ | QCISD/ VDZ | MP2/ VTZ | PBE0/ VTZ |
|---|---|---|---|---|---|---|---|---|
| $C_1$-$C_2$ | 1.547 | 1.553 | 1.553 | 1.555 | 1.552 | 1.553 | 1.554 | 1.556 |
| $C_2$-$C_3$ | 1.550 | 1.555 | 1.556 | 1.557 | 1.555 | 1.557 | 1.556 | 1.558 |
| $\angle C_1C_2C_3$ | 114.7 | 114.2 | 114.2 | 114.0 | 114.2 | 114.1 | 114.1 | 113.9 |
| $\angle C_2C_3C_4$ | 113.9 | 113.7 | 113.2 | 113.2 | 113.4 | 113.4 | 113.2 | 113.1 |
| $C_1C_2C_3C_4$ | 16.7 | 15.9 | 17.5 | 17.0 | 17.3 | 17.7 | 16.8 | 16.7 |
| Helical Angle | 14.0 | 13.3 | 14.6 | 14.2 | 14.2 | 14.8 | 14.1 | 14.0 |
| Std. Dev./ uÅ$^2$ | 0.28 | 0.071 | 0.060 | 0.23 | 0.16 | 0.13 | 0.036 | 0.050 |

**$C_6F_{14}$.** The lowest energy all trans conformer of n-hexane ($C_{2h}$) lacks a dipole moment and is therefore unobservable spectroscopically. A figure of the helical structure of $C_6F_{14}$, similar to Figure 3, given in reference 14 sparked our interest as this structure clearly has a dipole moment. The helicity of perfluoroalkanes results in structures with overall $C_2$ symmetry. For an odd numbered chain, like $C_5F_{12}$, the $C_2$ axis corresponds to the b-axis and b-type transitions are observed. For an even numbered chain the $C_2$ axis becomes the c-axis and, thus, c-type transitions are expected for $C_6F_{14}$. The observation and assignment of the microwave spectrum of $C_6F_{14}$ to c-type transitions unambiguously shows that the lowest energy structure of $C_6F_{14}$ is helical.

The structure of $C_3F_8$ was recently determined to be non-helical ($C_{2v}$).[15] The $P_{cc}$ second moment is 134.338 uÅ$^2$, or 44.78 uÅ$^2$ per $CF_2/CF_3$ group. Assuming transferability, $C_5F_{12}$ would have a $P_{cc}$ of 5 x 44.78 or 223.90 uÅ$^2$ if it retained $C_{2v}$ symmetry and $C_6F_{14}$ would have a $P_{cc}$ of 6 x 44.78 or 268.68 uÅ$^2$ if it exhibited $C_{2h}$ symmetry. The observed $P_{cc}$ for $C_5F_{12}$ is 229.616 uÅ$^2$, or 45.92 uÅ$^2$ per $CF_2/CF_3$ group. For $C_6F_{14}$ $P_{cc}$ is 281.857 uÅ$^2$, or 46.98 uÅ$^2$ per $CF_2/CF_3$ group. This increase in $P_{cc}$ also confirms the helical structures of $C_5F_{12}$ and $C_6F_{14}$ because C atoms as well as F atoms lie outside the ab plane and contribute to $P_{cc}$. The $P_{cc}$ second moment increases steadily as the C chain becomes longer. The $P_{cc}$ per $CF_2/CF_3$ group for $C_3F_8$[15] is 44.78 u Å$^2$ and is predicted to be 45.16 u Å$^2$ for $C_4F_{10}$ (from PBE0/VTZ calculations). This value increases to 45.92 uÅ$^2$ for $C_5F_{12}$ and to 46.98 uÅ$^2$ for $C_6F_{14}$. The trend demonstrates that as the C chain length increases more mass is displaced outside the ab plane and contributes to $P_{cc}$ due to the helicity of the structures.

To analyze the structural parameters of $C_6F_{14}$, the principal coordinates of the PBE0/VTZ computed model were scaled by the square root of the ratio of the observed second moments to the computed second moments, as described previously. The scale factors are 0.99996 for the a-coordinates, 1.00167 for the b-coordinates, and 1.00288 for the c-coordinates. Since the scale factors are nearly equal to 1, the structural parameters do not change much from the computed model (Table 4). The overall $C_2$ symmetry of $C_6F_{14}$ allows for two distinct dihedral angles. The exterior $C_1C_2C_3C_4$ dihedral angle (also equal to $C_3C_4C_5C_6$) is 16.7$^o$ away from trans and the interior $C_2C_3C_4C_5$ dihedral angle is 18.0$^o$ away from trans using this scaling approach. The exterior dihedral angle is in

agreement with the single dihedral angle of about 17° from trans determined in $C_5F_{12}$. The interior dihedral angle is slightly larger than the exterior dihedral angle likely because the interior of the molecule is more sterically crowded.

The scaled $C_6F_{14}$ structure was converted to helical parameters using Equations 1 and 2 above, averaging bond lengths, bond angles, and the dihedral angles. The helical radius ρ is 0.434 Å, the helical angle θ is 14.3°, and the pitch d is 1.298 Å. These values are in reasonable agreement with the 0.42 Å helical radius, 13.8° helical angle, and 1.292 Å pitch of the low temperature phase II form of PTFE[3] and are similar to those obtained for $C_5F_{12}$.

## Summary

The helical structures of $C_5F_{12}$ and $C_6F_{14}$ have been observed and assigned by their microwave rotational spectra. The structural parameters were characterized by the scaling of computed models to exactly reproduce the observed second moments. The scaled structures of $C_5F_{12}$ result in a $C_1C_2C_3C_4$ dihedral angle of 17° ± 1° away from trans. The $C_1C_2C_3C_4$ exterior dihedral angle is 16.7° from trans and the $C_2C_3C_4C_5$ interior dihedral angle is 18.0° from trans in $C_6F_{14}$ from a scaled PBE0/VTZ model. In terms of helical parameters the helical angle of both $C_5F_{12}$ and $C_6F_{14}$ is about 14°, in good agreement with the 13.8° helical angle of the low temperature phase II form of PTFE.

## References


[1] Bunn, C.W.; Howells, E.R. *Nature* **1954**, *174*, 549.
[2] Shimanouchi, T.; Mizushima, S. *J. Chem. Phys.* **1955**, *23*, 707.
[3] Iwasaki, M. *J. Polym. Sci.* **1963**, *A-1*, 1099.
[4] Sperati, C.A.; Starkweather, H.W., Jr. *Fortschr. Hochpolym. Forsch.* **1961**, *2*, 465.
[5] Zhang, W. P.; Dorset, D. L. *Macromolecules* **1990**, *23*, 4322.
[6] Dixon, D.A. *J. Phys. Chem.* **1992**, *96*, 3698
[7] Smith, G.D.; Jaffe, R.L.; Yoon, D.Y. *Macromolecules* **1994**, *27*, 3166.
[8] Albinsson, B.; Michl, J. *J. Phys. Chem.* **1996**, *100*, 3418.
[9] Röthlisberger, U.; Laasonen, K.; Klein, M.L.; Sprik, M. *J. Chem. Phys.* **1996**, *104*, 3692.
[10] Watkins, E.K.; Jorgensen, W.L. *J. Phys. Chem.* A **2001**, *105*, 4118.
[11] Borodin, O.; Smith, G.D.; Bedrov, D. *J. Phys. Chem. B* **2002**, *106*, 9912.
[12] Ignatieva, L.N.; Beloiptsev, A.Y.; Kozlova, S.G. *J. Struct. Chem.* **2004**, *45*, 599.

[13] D'Amore, M.; Talarico, G.; Barone, V. *J. Am. Chem. Soc.* **2006,** *128*, 1099.
[14] Golden, W.G.; Brown, E.M.; Solem, S.E.; Zoellner, R.W. *J. Mol. Spectrosc.* **2008**, *867*, 22.
[15] Fournier, J.A.; Bohn, R.K.; Montgomery, J.A., Jr.; Onda, M. *J. Phys. Chem. A* **2010**, *114*, 1118.
[16] Munrow, M.R.; Subramanian, R.; Minei, A.J.; Antic, D.; MacLeod, M.K.; Michl, J.; Crespo, R.; Piqueras, M.C.; Izuha, M; Ito, T.; Tatamitani, Y.; Yamanou, K.; Ogata, T.; Novick, S.E. *J. Mol. Spectrosc.* **2007**, *242*, 129.
[17] Ruoff, R.; Klots, T.; Emilsson, T.; Gutowsky, H. *J. Phys. Chem*. **1990**, *93*, 3142.
[18] Balle, T.J.; Flygare, W.H. *Rev. Sci. Instr.* **1981**, *52*, 33.
[19] Hight-Walker, A.R.; Lou, Q.; Bohn, R.K.; Novick, S.E. *J. Molec. Struct.* **1995**, *346*, 187.
[20] J. K. G. Watson, in *Vibrational Spectra and Structure*, Vol. 6 (J. R. Durig, Ed.), Elsevier, Amsterdam, pp 1-89, 1977.
[21] Pickett, H.M. *J. Mol. Spectrosc.* **1991**, *148*, 371.
[22] Gaussian 03, Revision B.05, M. J. Frisch, G. W. Trucks, H. B. Schlegel, G. E. Scuseria, M. A. Robb, J. R. Cheeseman, J. A. Montgomery, Jr., T. Vreven, K. N. Kudin, J. C. Burant, J. M. Millam, S. S. Iyengar, J. Tomasi, V. Barone, B. Mennucci, M. Cossi, G. Scalmani, N. Rega, G. A. Petersson, H. Nakatsuji, M. Hada, M. Ehara, K. Toyota, R. Fukuda, J. Hasegawa, M. Ishida, T. Nakajima, Y. Honda, O. Kitao, H. Nakai, M. Klene, X. Li, J. E. Knox, H. P. Hratchian, J. B. Cross, C. Adamo, J. Jaramillo, R. Gomperts, R. E. Stratmann, O. Yazyev, A. J. Austin, R. Cammi, C. Pomelli, J. W. Ochterski, P. Y. Ayala, K. Morokuma, G. A. Voth, P. Salvador, J. J. Dannenberg, V. G. Zakrzewski, S. Dapprich, A. D. Daniels, M. C. Strain, O. Farkas, D. K. Malick, A. D. Rabuck, K. Raghavachari, J. B. Foresman, J. V. Ortiz, Q. Cui, A. G. Baboul, S. Clifford, J. Cioslowski, B. B. Stefanov, G. Liu, A. Liashenko, P. Piskorz, I. Komaromi, R. L. Martin, D. J. Fox, T. Keith, M. A. Al-Laham, C. Y. Peng, A. Nanayakkara, M. Challacombe, P. M. W. Gill, B. Johnson, W. Chen, M. W. Wong, C. Gonzalez, and J. A. Pople, Gaussian, Inc., Pittsburgh PA, 2003.
[23] Kraitchman, J. *Am. J. Phys*. **1953**, *21*, 17.

# Chapter 5. Two Conformers of 1H-heptafluoropropane and the $C_{2v}$ Conformer of Perfluoropropane

## Introduction

Fluorocarbons and hydrofluorocarbons (HFCs) are important industrial materials that have come under scrutiny in recent years due to their potency as greenhouse gases. The polymer polytetrafluoroethylene (PTFE, Teflon©) has been studied extensively using X-ray diffraction on single fibers and determined to have a helical structure.[1] The carbon backbone dihedral angle is periodic and twisted about 17° away from trans in the low

temperature phase II form.[2] Computational studies on smaller perfluoroalkane oligomers also predict helical structures for the lowest energy all trans conformations.[3-11] Recent microwave studies of perfluoropentane ($C_5F_{12}$) and perfluorohexane ($C_6F_{14}$) confirms helical structures with CCCC dihedral angles of ~17° from trans.[12] This helicity has been attributed to steric and dipole repulsions between fluorine atoms on alternate carbons.

HFCs are used as refrigerants and propellants, and have replaced chlorofluorocarbons (CFCs) because they do not degrade ozone in the atmosphere. HFCs have also found medicinal applications such as the propellants in inhalers. Fluorocarbons, which dissolve large amounts of oxygen, have been studied as possible blood substitutes. Several HFCs have been characterized by microwave spectroscopy, including 1,1,1,2,3,3,3-heptafluoropropane,[13] 2,2-difluoropropane,[14] and 1,1,1,3,3,3-hexafluoropropane.[15] Each exists in a single conformation.

In this study, the rotational spectra and structures of the $C_{2v}$ conformer of perfluoropropane ($C_3F_8$) and two conformers of 1,1,2,2,3,3,3-heptafluoropropane (1H-heptafluoropropane, HFP) are analyzed. The $HC_1C_2C_3$ dihedral angle in HFP is analogous to that in butane and is expected to exhibit both trans and gauche conformations (Figures 1 and 2). The microwave spectra of both conformers have been observed and assigned and the structures analyzed by the scaling of computed models.

Figure 1. The gauche (left) and trans (center) conformers of HFP and the $C_{2v}$ conformer of $C_3F_8$ (right) looking along the b-axis.

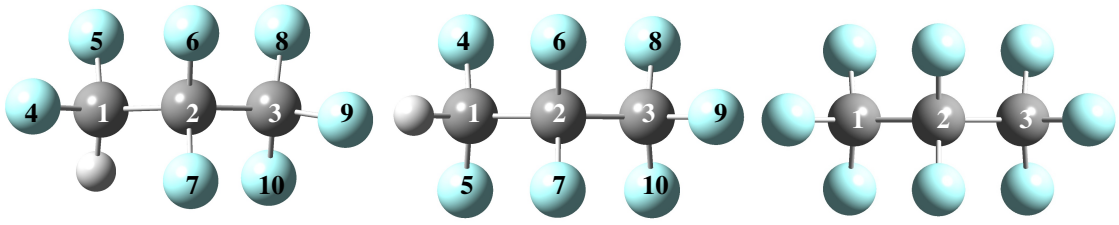

Figure 2. The gauche (left) and trans (center) conformers of HFP and the $C_{2v}$ conformer of $C_3F_8$ (right) looking along the a-axis. The $HC_1C_2C_3$ dihedral angle for the trans conformer of HFP is 180°.

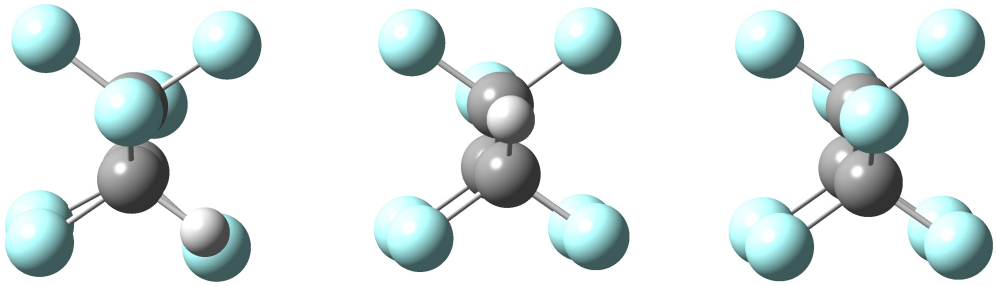

## Experimental

**HFP.** HFP was purchased from Synquest Laboratories and used directly. Vapor of the sample was transferred into a 2 L tank to a pressure of 0.049 atm and 4.9 atm He was added to produce a 1% sample mixture. Pulses of the sample mixture at 2.5 atm were admitted at 5 Hz into the nozzle of the pulsed-jet Fourier Transform microwave spectrometer[16] of the Southern New England Microwave Consortium.[17] Five microwave pulses were observed per gas pulse and rotational transitions were observed in the range between 7 and 15 GHz although the complete range was not scanned. The rotational temperature of the expanded gas is estimated to be ~3 K. Transitions were observed as Doppler doublets and line widths in the power spectrum ranged from 10-20 kHz with uncertainties estimated to be about 2 kHz.

**$C_3F_8$.** The $C_3F_8$ measurements were carried out at Sophia University using a pulsed-jet Fourier transform microwave spectrometer.[16,18,19] The sample was purchased from Synquest Laboratories and used directly. The sample was mixed with argon to a concentration of about 2%. Rotational transitions were observed in the 6 – 16 GHz range.

## Results

**HFP.** Rotational constants for the gauche and trans conformers of HFP were predicted from MP2/6-31G* *ab initio* models using the *Gaussian 03* program[20] and rotational

transitions were predicted using the Pickett suite of programs.[21] A rich array of transitions were observed in the 9.2 – 11.3 GHz range. The spectral fitting program jb95[22] was used to tentatively assign the observed transitions. The rotational constants in jb95 were adjusted to match a Q-branch for the gauche conformer with a band head at 10348 MHz corresponding to $\Delta K_p$ of 6←5. Other lines matched predicted transitions and a complete assignment for the gauche conformer was made. Additional lines were predicted and measured. A total of 71 transitions were observed of which 8 are a-types, 18 are b-types, and 45 are c-types. The observation of lines with all three types of selection rules indicates that the conformer has $C_1$ symmetry. The lines were fit to an rmsd of 1.1 kHz using rotational constants and 5 quartic centrifugal distortion constants using Watson's A reduction in the $I^r$ representation.[23] The spectroscopic constants are displayed in Table 1 and the observed transitions are in Supplementary Table 6.

A pair of very intense lines at 9922 and 9925 MHz were close to the predicted $3_{31}$-$2_{20}$/$3_{30}$-$2_{21}$ transitions for the trans conformer. The rotational constants in jb95 were adjusted to match these two transitions and about a dozen more lines fell into place. A complete assignment was made, and more lines were predicted and measured. 38 lines were measured of which 12 are a-types and 26 are b-types. A search for c-type transitions, which would be expected if the trans form had a helical twist, was unsuccessful. The observation of only a- and b-types lines indicates the trans form has $C_s$ symmetry and lacks a c-dipole due to an ab plane of symmetry. The lines were fit to a rmsd of 1.7 kHz using rotational constants and 5 quartic centrifugal distortion constants using Watson's A reduction[23] in the $I^r$ representation (Table 1). The measured transitions are displayed in Supplementary Table 7.

**$C_3F_8$.** Spectroscopic constants for $C_3F_8$ are displayed in Table 1 and the complete list of observed lines is provided in Supplementary Table 7. The experimental constants provide no information about a helical $C_2$ structure vs. a non-helical $C_{2v}$ structure.

Rotational constants and second moments for $C_3F_8$ predicted at the MP2/VTZ and PBE0/VTZ level are in excellent agreement with the observed. Unlike other perfluoroalkanes, computations predict the $C_{2v}$ non-helical form to be the lowest energy

structure of $C_3F_8$. Apparently the postulated fluorine steric and dipole repulsions are insufficient in a three-carbon chain to distort the trans geometry into a helical form.

Table 1. Spectroscopic constants of the gauche and trans conformer of HFP, and $C_3F_8$.

| | HFP Gauche | HFP Trans | $C_3F_8$ |
|---|---|---|---|
| A/MHz | 1995.4656(7) | 1752.4998(10) | 1678.5982(9) |
| B/MHz | 1120.2799(4) | 1184.3437(19) | 955.3216(11) |
| C/MHz | 982.7300(5) | 1137.0414(20) | 900.1968(10) |
| $\Delta_J$/kHz | 0.0691(4) | 0.0938(20) | |
| $\Delta_{JK}$/kHz | 0.0315(11) | 0.763(10) | |
| $\Delta_K$/kHz | 0.0378(14) | -0.758(8) | |
| $\delta_J$/kHz | 0.01578(19) | 0.0092(18) | |
| $\delta_K$/kHz | -0.238(3) | -1.12(8) | |
| $D_J$/kHz | | | 0.046(24) |
| $D_{JK}$/kHz | | | 0.18(6) |
| $D_K$/kHz | | | 0.15(4) |
| $P_{aa}$/uÅ$^2$ | 356.060 | 291.405 | 394.676 |
| $P_{bb}$/uÅ$^2$ | 158.205 | 153.064 | 166.734 |
| $P_{cc}$/uÅ$^2$ | 95.059 | 135.312 | 134.339 |
| Kappa | -0.728360 | -0.846284 | -0.858364 |
| No. Lines | 71 | 38 | 17 |
| rmsd/kHz | 1.1 | 1.7 | 0.5 |

## Discussion

**HFP.** The $HC_1C_2C_3$ backbone of HFP is analogous to the CCCC dihedral angle in butane and is expected to have both trans and gauche orientations. This expectation was confirmed. The exact $HC_1C_2C_3$ dihedral angle for the trans form is of interest since perfluoroalkanes, like PTFE, exhibit helical structures with CCCC dihedral angles about 17$^o$ away from trans.[1-12] The helical structure of perfluoroalkanes has been attributed to steric and dipole repulsions between fluorine atoms on alternate carbons. However, computational results on $C_3F_8$ predict the structure to be $C_{2v}$ and not helical ($C_2$). The experimental results do not reveal any information about the dihedral angle due to the three-fold symmetry of the terminal $CF_3$ groups. The substitution of one fluorine by hydrogen in HFP allows for a distinct determination of the $HC_1C_2C_3$ orientation by breaking the symmetry of one $CF_3$ group. A helical twist would allow c-type transitions

whereas a trans structure would not allow c-types due to an ab-plane of symmetry. An extensive search for c-type lines was performed, but none were observed. Therefore, the $HC_1C_2C_3$ dihedral angle for the trans conformer of HFP is either $180^o$ or so slightly twisted that the c-dipole is not sufficiently large to observe c-type transitions.

Structural analysis was performed by scaling PBE0/VTZ computed models. The PBE0 hybrid functional has been shown to accurately model perfluoroalkanes.[10,12] Our PBE0/VTZ results for both the gauche and trans conformers are in excellent agreement with the observed spectroscopic constants (Table 2). The principal coordinates from these computed models were scaled by the square root of the ratio of the observed second moments to the computed second moments. These scale factors shift the coordinates of each atom to exactly reproduce the observed second moments. The scale factors for the gauche form are 1.00033 for the a-coordinates, 1.00268 for the b-coordinates, and 1.00122 for the c-coordinates. Since the scale factors are close to 1 the atoms are shifted only slightly and the scaled structural parameters are minutely different from the computed model (Table 3). The scaled $HC_1C_2C_3$ dihedral angle of the gauche form is $60.9^o$.

A similar scaling was performed for the trans conformer. The scaling factors are 0.99941 for the a-coordinates, 1.00316 for the b-coordinates, and 1.00148 for the c-coordinates. These factors are again close to 1 so the scaled structure is not significantly different from the computed model. The computed model gives a $HC_1C_2C_3$ dihedral angle of exactly $180^o$. Since the computed structure has $C_s$ symmetry, the scaled model also assumes a $C_s$ structure (Table 3). The highly accurate reproduction of observed values by the PBE0/VTZ computation and the absence of c-type lines strongly indicate that the trans form does have an ab-plane of symmetry with a $HC_1C_2C_3$ dihedral angle of $180^o$.

Both conformers show very strong transitions with comparable intensities, evidence that the energy difference between the forms is small. The PBE0/VTZ calculations predict the gauche form to be negligibly lower in energy (Table 2). The gauche form has one fluorine on $C_1$ eclipsed with a fluorine on $C_3$ whereas the trans form as two fluorine atoms on $C_1$ eclipsed with two fluorine atoms on $C_3$ (Figures 1 and 2). Intuitively, the gauche form is expected to be lower in energy due to one fewer F-F

interaction. The presence of the additional interaction in the trans form can be seen in the differing bond angles. The scaled $C_1C_2C_3$ bond angle for the gauche form is 113.9° and is 116.9° for the trans form. The two C-C bond lengths are nearly equal for both forms, so the increased $C_1C_2C_3$ bond angle in the trans conformer can likely be attributed to the alleviation of steric repulsions between the eclipsed fluorine atoms on $C_1$ and $C_3$.

Table 2. Comparison of observed spectroscopic constants to computed and scaled PBE0/VTZ models of HFP.

| | Gauche | | | Trans | | |
|---|---|---|---|---|---|---|
| | Obs'd | PBE0/VTZ | Scaled PBE0/VTZ | Obs'd | PBE0/VTZ | Scaled PBE0/VTZ |
| A/MHz | 1995.4656 | 2004.0 | 1995.46 | 1752.4998 | 1760.8 | 1752.50 |
| B/MHz | 1120.2799 | 1121.4 | 1120.28 | 1184.3437 | 1184.5 | 1184.34 |
| C/MHz | 982.7300 | 984.8 | 982.72 | 1137.0414 | 1138.6 | 1137.04 |
| $P_{aa}$/uÅ$^2$ | 356.060 | 355.8 | 356.06 | 291.405 | 291.8 | 291.40 |
| $P_{bb}$/uÅ$^2$ | 158.205 | 157.4 | 158.21 | 153.064 | 152.1 | 153.06 |
| $P_{cc}$/uÅ$^2$ | 95.059 | 94.8 | 95.06 | 135.312 | 134.9 | 135.31 |
| Rel. Energy / kcal mol$^{-1}$ | | 0 | | | 0.07 | |

Table 3. Selected structural parameters of the computed and scaled PBE0/VTZ models of HFP.

| | Gauche | | Trans | |
|---|---|---|---|---|
| | PBE0/VTZ | Scaled PBE0/VTZ | PBE0/VTZ | Scaled PBE0/VTZ |
| $C_1$-$C_2$ | 1.536 | 1.538 | 1.535 | 1.535 |
| $C_2$-$C_3$ | 1.545 | 1.546 | 1.546 | 1.548 |
| $\angle C_1C_2C_3$ | 114.0 | 113.9 | 117.0 | 116.9 |
| $HC_1C_2C_3$ | 60.8 | 60.9 | 180 | 180 |
| $F_4C_1C_2C_3$ | 179.1 | 179.1 | 60.1 | 60.1 |
| $F_9C_3C_2C_1$ | 170.9 | 170.9 | 180 | 180 |

**$C_3F_8$.** The computed models of $C_3F_8$ were also scaled, as described above. The scaling ratios using the MP2/VTZ model were 1.0030 for the a-coordinate, 1.0018 for the b-coordinate, and 0.9993 for the c-coordinate, respectively. Like HFP, the scaled molecular parameters are only slightly changed from the computed structure (Table 5). The scaled C-C bond length is 1.544Å, similar to the $C_2$-$C_3$ bond lengths in both the gauche and trans forms of HFP. The $C_1$-$C_2$ bond lengths in HFP are about 0.01 Å shorter

than the $C_2$-$C_3$ bond lengths due to the replacement of one F atom by H. The scaled CCC bond angle in $C_3F_8$ is 115.7°, in between the CCC bond angles of the gauche and trans forms of HFP. The gauche conformer has one fewer F-F interaction than the trans conformer and $C_3F_8$, thus a larger bond angle is not required to alleviate the steric interactions. The trans conformer has a shorter $C_1$-$C_2$ bond length compared to $C_3F_8$, so an increased bond angle helps alleviate the steric interactions between F atoms. As discussed previously, the structure of $C_3F_8$ has $C_{2v}$ symmetry and is not helical. It is apparent that the steric and dipole repulsions which determine the helical structure of longer perfluoroalkane oligomers are not sufficient to cause a twist in a three carbon chain.

Table 4. Comparison of observed spectroscopic constants to computed values for $C_3F_8$.

| | Obs'd | MP2/VTZ | PBE0/VTZ |
|---|---|---|---|
| A/MHz | 1678.5982 | 1680.9 | 1685.0 |
| B/MHz | 955.3216 | 959.2 | 956.5 |
| C/MHz | 900.1968 | 904.9 | 901.5 |
| $P_{aa}$/uÅ$^2$ | 394.676 | 392.3 | 394.5 |
| $P_{bb}$/uÅ$^2$ | 166.734 | 166.1 | 166.1 |
| $P_{cc}$/uÅ$^2$ | 134.339 | 134.5 | 133.8 |

Table 5. Comparison of selected scaled and computed structural parameters of $C_3F_8$.

| Parameter | MP2/VTZ | Scaled MP2/VTZ | PBE0/VTZ | Scaled PBE0/VTZ |
|---|---|---|---|---|
| $C_1$-$C_2$ | 1.544 | 1.544 | 1.549 | 1.550 |
| $C_2$-$C_3$ | 1.544 | 1.544 | 1.549 | 1.550 |
| $\angle C_1C_2C_3$ | 115.7 | 115.7 | 115.7 | 115.6 |
| $\angle C_2C_3C_4$ | 115.7 | 115.7 | 115.7 | 115.6 |

## Summary

The microwave spectra of two conformers of 1H-heptafluoropropane and the $C_{2v}$ conformer of perfluoropropane have been observed and assigned. The $HC_1C_2C_3$ dihedral angle in HFP exhibits trans and gauche conformations which are very close in energy. The structures were characterized by scaling the principal coordinates of computed

models. The scaled structures exactly reproduce the observed second moments and are not significantly different from the computed models. From this scaling approach, the $HC_1C_2C_3$ dihedral angle for the gauche form of HFP is about 61° and that of the trans form is exactly 180°. The structure of $C_3F_8$ appears to be non-helical ($C_{2v}$). It is apparent that the F-F steric and dipole interactions on alternate carbons are not sufficient to cause a helical twist in a three carbon chain or that factors other than simple steric repulsions determine the structures of fluoroalkanes. HFCs are important industrial materials and have gained attention for their greenhouse gas capabilities. Few HFCs have been structurally characterized,[13-15] and HFP is the first with multiple conformations.

**Reference**


[1] Bunn, C.W.; Howells, E.R. *Nature* **1954**, *174*, 549.
[2] Sperati, C.A.; Starkweather, H.W., Jr. *Fortschr. Hochpolym. Forsch.* **1961**, *2*, 465.
[3] Dixon, D.A. *J. Phys. Chem.* **1992**, *96*, 3698
[4] Smith, G.D.; Jaffe, R.L.; Yoon, D.Y. *Macromolecules* **1994**, *27*, 3166.
[5] Albinsson, B.; Michl, J. *J. Phys. Chem.* **1996**, *100*, 3418.
[6] Röthlisberger, U.; Laasonen, K.; Klein, M.L.; Sprik, M. *J. Chem. Phys.* **1996**, *104*, 3692.
[7] Watkins, E.K.; Jorgensen, W.L. *J. Phys. Chem.* A **2001**, *105*, 4118.
[8] Borodin, O.; Smith, G.D.; Bedrov, D. *J. Phys. Chem. B* **2002**, *106*, 9912.
[9] Ignatieva, L.N.; Beloiptsev, A.Y.; Kozlova, S.G. *J. Struct. Chem.* **2004**, *45*, 599.
[10] D'Amore, M.; Talarico, G.; Barone, V. *J. Am. Chem. Soc.* **2006,** *128*, 1099.
[11] Golden, W.G.; Brown, E.M.; Solem, S.E.; Zoellner, R.W. *J. Mol. Spectrosc.* **2008**, *867*, 22.
[12] Fournier, J.A.; Bohn, R.K.; Montgomery, J.A., Jr.; Onda, M. *J. Phys. Chem. A* **2010**, *114*, 1118.
[13] Heineking, N; Stahl, W.; Thomson, C. *J. Mol. Spectrosc.* **1991**, *146*, 402.
[14] Takeo, H.; Sugie, M.; Matsumura,C. *J. Mol. Struct.* **1995**, *352-353*, 267.
[15] Onda, M.; Tsuda, K.; Sakamoto, E. *J. Mol. Struct.* **2006**, *780-781*, 222.
[16] Balle, T.J.; Flygare, W.H. *Rev. Sci. Instr.* **1981**, *52*, 33.
[17] Hight-Walker, A.R.; Lou, Q.; Bohn, R.K.; Novick, S.E. *J. Molec. Struct.* **1995**, *346*, 187.
[18] Onda, M.; Tsuda, K.; Sakamoto, E. *J. Mol. Spectrosc*. **2006**, *780-781*, 222.
[19] Suenram, R.D.; Lovas, F.J.; Fraser, G.T.; Gillies, J.Z.; Gillies, C.W.; Onda, M. *J. Mol. Spectrosc.* **1989**, *137*, 127.
[20] Gaussian 03, Revision B.05, M. J. Frisch, G. W. Trucks, H. B. Schlegel, G. E. Scuseria, M. A. Robb, J. R. Cheeseman, J. A. Montgomery, Jr., T. Vreven, K. N. Kudin, J. C. Burant, J. M. Millam, S. S. Iyengar, J. Tomasi, V. Barone, B. Mennucci, M. Cossi, G. Scalmani, N. Rega, G. A. Petersson, H. Nakatsuji, M. Hada, M. Ehara, K. Toyota, R. Fukuda, J. Hasegawa, M. Ishida, T. Nakajima, Y. Honda, O. Kitao, H. Nakai, M. Klene, X. Li, J. E. Knox, H. P. Hratchian, J. B. Cross, C. Adamo, J. Jaramillo, R. Gomperts, R.

E. Stratmann, O. Yazyev, A. J. Austin, R. Cammi, C. Pomelli, J. W. Ochterski, P. Y. Ayala, K. Morokuma, G. A. Voth, P. Salvador, J. J. Dannenberg, V. G. Zakrzewski, S. Dapprich, A. D. Daniels, M. C. Strain, O. Farkas, D. K. Malick, A. D. Rabuck, K. Raghavachari, J. B. Foresman, J. V. Ortiz, Q. Cui, A. G. Baboul, S. Clifford, J. Cioslowski, B. B. Stefanov, G. Liu, A. Liashenko, P. Piskorz, I. Komaromi, R. L. Martin, D. J. Fox, T. Keith, M. A. Al-Laham, C. Y. Peng, A. Nanayakkara, M. Challacombe, P. M. W. Gill, B. Johnson, W. Chen, M. W. Wong, C. Gonzalez, and J. A. Pople, Gaussian, Inc., Pittsburgh PA, 2003.

[21] Pickett, H.M. *J. Mol. Spectrosc.* **1991**, *148*, 371.

[22] Plusquellic, D.F.; Suenram, R.D.; Mate, B.; Jensen, J.O.; Samuels, A.C. *J. Chem. Phys.* **2001**, *115*, 3057.

[23] J. K. G. Watson, in *Vibrational Spectra and Structure*, Vol. 6 (J. R. Durig, Ed.), Elsevier, Amsterdam, pp 1-89, 1977.

## Acknowledgments

The author would like to thank his advisor, Prof. Robert Bohn, for his guidance and mentorship over the past three and a half years. Prof. Harvey Michels and Prof. John Montgomery, Jr. taught and guided the author on computational methods and provided invaluable insights. Their time and effort is much appreciated. The author would also like to thank his fellow undergraduate students in the Bohn group, James Dombrowski and Congtin Phan.

All experiments were performed using the pulsed-jet Fourier transform microwave spectrometer of the Southern New England Microwave Consortium at Wesleyan University. The author would like to thank Prof. Stewart Novick, Prof. Pete Pringle, Andrei Minei, and Dan Frohman of Wesleyan University for generous assistance with the spectrometer and for stimulating conversation and scientific insight.

The author is very grateful for the support of his family and friends during the last four years at the University of Connecticut. He is especially thankful for his mother's support, without which his academic and scientific accomplishment would not have been possible. All these individuals have made the author's time at the University of Connecticut very memorable.

# Appendix I. Supplementary Material

Supplementary Table 1. Observed transitions for the two conformers of 6-methyl-3-heptyne.

| J' | $K_p$' | $K_o$' | ← | J'' | $K_p$'' | $K_o$'' | $C_s$ Freq/MHz | $C_s$ (Obs-Calc)/kHz | $C_1$ Freq/MHz) | $C_1$ (Obs-Calc)/kHz |
|---|---|---|---|---|---|---|---|---|---|---|
| a-type | | | | | | | | | | |
| 5 | 0 | 5 | | 4 | 0 | 4 | 9123.6380 | 0.2 | | |
| 5 | 1 | 5 | | 4 | 1 | 4 | 8998.9362 | -0.2 | | |
| 5 | 1 | 4 | | 4 | 1 | 3 | 9279.0711 | -0.9 | | |
| 6 | 0 | 6 | | 5 | 0 | 5 | 10937.4529 | 0.2 | | |
| 6 | 1 | 6 | | 5 | 1 | 5 | 10795.9918 | -0.9 | | |
| 6 | 1 | 5 | | 5 | 1 | 4 | 11131.7459 | -1.8 | | |
| 7 | 0 | 7 | | 6 | 0 | 6 | 12745.6107 | 0.0 | | |
| 7 | 1 | 7 | | 6 | 1 | 6 | 12591.6599 | 0.1 | | |
| 7 | 1 | 6 | | 6 | 1 | 5 | | | 10859.4916 | 4.1 |
| 7 | 2 | 5 | | 6 | 2 | 4 | | | 10649.2682 | -0.9 |
| 8 | 0 | 8 | | 7 | 0 | 7 | | | 11982.4123 | 1.2 |
| 8 | 2 | 7 | | 7 | 2 | 6 | | | 12078.7916 | 1.1 |
| 8 | 3 | 6 | | 7 | 3 | 5 | | | 12110.6406 | -0.5 |
| 8 | 3 | 5 | | 7 | 3 | 4 | | | 12114.1993 | -1.3 |
| 12 | 1 | 12 | | 11 | 1 | 11 | | | 17553.9216 | -1.4 |
| b-type | | | | | | | | | | |
| 4 | 1 | 4 | | 3 | 0 | 3 | 9405.1816 | -2.6 | | |
| 5 | 1 | 5 | | 4 | 0 | 4 | 11099.1878 | 0.5 | 10787.1346 | -1.9 |
| 6 | 1 | 6 | | 5 | 0 | 5 | 12771.5438 | 1.7 | 12063.2467 | 0.8 |
| 7 | 1 | 7 | | 6 | 0 | 6 | 14425.7507 | 1.4 | | |
| 8 | 1 | 8 | | 7 | 0 | 7 | 16065.9268 | 1.2 | 14536.3698 | -0.1 |
| 9 | 1 | 9 | | 8 | 0 | 8 | 17696.6336 | -2.5 | | |
| 11 | 1 | 11 | | 10 | 0 | 10 | | | 18143.2583 | 2.8 |
| 6 | 0 | 6 | | 5 | 1 | 5 | 8961.9034 | 0.2 | | |
| 7 | 0 | 7 | | 6 | 1 | 6 | 10911.5238 | 2.5 | | |
| 8 | 0 | 8 | | 7 | 1 | 7 | 12867.4036 | -4.5 | | |
| 9 | 0 | 9 | | 8 | 1 | 8 | 14824.5928 | -1.1 | 10894.2090 | 0.8 |
| 10 | 0 | 10 | | 9 | 1 | 9 | 16778.2762 | 1.3 | | |
| 13 | 0 | 13 | | 12 | 1 | 12 | | | 17671.0473 | -1.0 |
| 2 | 2 | 1 | | 1 | 1 | 0 | 10734.9308 | -1.7 | 14524.9267 | -2.1 |
| 3 | 2 | 2 | | 2 | 1 | 1 | 12507.3353 | -3.7 | 15952.6964 | -3.6 |
| 4 | 2 | 3 | | 3 | 1 | 2 | 14251.4228 | -2.8 | 17338.1428 | 0.4 |
| 5 | 2 | 4 | | 4 | 1 | 3 | 15967.2789 | 4.4 | 18681.3977 | -0.2 |
| 6 | 2 | 5 | | 5 | 1 | 4 | 17655.0846 | -0.7 | | |

| | | | | | | | | | |
|---|---|---|---|---|---|---|---|---|---|
| 7 | 2 | 6 | 6 | 1 | 5 | 19315.2027 | 3.9 | | |
| 2 | 2 | 0 | 1 | 1 | 1 | 10792.0328 | 0.9 | 14610.5557 | -0.8 |
| 3 | 2 | 1 | 2 | 1 | 2 | 12680.6340 | -2.0 | | |
| 4 | 2 | 2 | 3 | 1 | 3 | 14602.9993 | 9.1 | 17864.3126 | 4.4 |
| 5 | 2 | 3 | 4 | 1 | 4 | 16563.0677 | 2.3 | | |
| 6 | 2 | 4 | 5 | 1 | 5 | 18565.7615 | 1.1 | | |
| 3 | 3 | 1 | 2 | 2 | 0 | 17328.0426 | -4.1 | | |
| 4 | 3 | 2 | 3 | 2 | 1 | 19154.1910 | -3.0 | | |
| 3 | 3 | 0 | 2 | 2 | 1 | 17329.0609 | -0.4 | | |
| 4 | 3 | 1 | 3 | 2 | 2 | 19159.2851 | -2.6 | | |
| 3 | 2 | 1 | 3 | 1 | 2 | | | 11298.1350 | -2.9 |
| 4 | 2 | 2 | 4 | 1 | 3 | | | 11145.2322 | -2.9 |
| 5 | 2 | 3 | 5 | 1 | 4 | | | 10965.3592 | -0.2 |
| 6 | 2 | 4 | 6 | 1 | 5 | | | 10765.9399 | -0.1 |
| 5 | 2 | 4 | 5 | 1 | 5 | | | 12180.3308 | 7.1 |
| 5 | 3 | 3 | 5 | 2 | 4 | 11850.5538 | -0.9 | | |
| 6 | 3 | 4 | 6 | 2 | 5 | 11859.7284 | -1.1 | | |
| 7 | 3 | 5 | 7 | 2 | 6 | 11874.5467 | 0.4 | | |
| 8 | 3 | 6 | 8 | 2 | 7 | 11896.7485 | 1.2 | | |
| 5 | 3 | 2 | 5 | 2 | 3 | 11815.8830 | -0.4 | | |
| 6 | 3 | 3 | 6 | 2 | 4 | 11790.9455 | 0.4 | | |
| 7 | 3 | 4 | 7 | 2 | 5 | 11752.0683 | -0.7 | | |
| 8 | 3 | 5 | 8 | 2 | 6 | 11695.4922 | -0.3 | | |
| 11 | 3 | 8 | 11 | 2 | 9 | | | 18606.8775 | 2.2 |
| 12 | 3 | 9 | 12 | 2 | 10 | | | 18385.8565 | -1.5 |
| 14 | 3 | 11 | 14 | 2 | 12 | | | 17826.0358 | -2.0 |
| 15 | 3 | 12 | 15 | 2 | 13 | | | 17494.6796 | 0.2 |
| 4 | 4 | 1 | 4 | 3 | 2 | 16577.5225 | -4.5 | | |
| 5 | 4 | 2 | 5 | 3 | 3 | 16575.7421 | -4.7 | | |
| 6 | 4 | 3 | 6 | 3 | 4 | 16573.1363 | -4.7 | | |
| 7 | 4 | 4 | 7 | 3 | 5 | 16569.5497 | -1.4 | | |
| 8 | 4 | 5 | 8 | 3 | 6 | 16564.8680 | -1.2 | | |
| 9 | 4 | 6 | 9 | 3 | 7 | 16559.0690 | 0.7 | | |
| 4 | 4 | 0 | 4 | 3 | 1 | 16577.4605 | 12.9 | | |
| 5 | 4 | 1 | 5 | 3 | 2 | 16575.4330 | 3.4 | | |
| 6 | 4 | 2 | 6 | 3 | 3 | 16572.1949 | 2.8 | | |
| 7 | 4 | 3 | 7 | 3 | 4 | 16567.1879 | 0.7 | | |
| 8 | 4 | 4 | 8 | 3 | 5 | 16559.6909 | -0.7 | | |
| c-type | | | | | | | | | |
| 8 | 1 | 7 | 7 | 0 | 7 | | | 17562.3551 | -1.7 |
| 2 | 2 | 0 | 1 | 1 | 0 | | | 14526.3127 | 0.9 |
| 3 | 2 | 1 | 2 | 1 | 1 | | | 15959.6089 | -3.3 |
| 4 | 2 | 2 | 3 | 1 | 2 | | | 17358.8590 | -1.8 |

| | | | | | | |
|---|---|---|---|---|---|---|
| 2 | 2 | 1 | 1 | 1 | 1 | 14609.1730 | -0.6 |
| 3 | 2 | 2 | 2 | 1 | 2 | 11291.2252 | -0.5 |
| 4 | 2 | 3 | 3 | 1 | 3 | 17843.5898 | 0.0 |
| 4 | 2 | 3 | 4 | 1 | 3 | 11124.5173 | 0.6 |
| 5 | 2 | 4 | 5 | 1 | 4 | 10917.0984 | 0.5 |
| 6 | 2 | 5 | 6 | 1 | 5 | 10669.6998 | 5.5 |
| 11 | 3 | 9 | 11 | 2 | 9 | 18564.7346 | 1.0 |

Supplementary Table 2. Assigned transitions for the three conformers of 2-methylpentane.

| J' | $K_p$' | $K_o$' | ← | J" | $K_p$" | $K_o$" | Freq/MHz $C_s$ (AA) | (Obs-Calc)/kHz $C_s$ (AA) | Freq/MHz $C_1$ (AG) | (Obs-Calc)/kHz $C_1$ (AG) | Freq/MHz $C_1$ (GG) | (Obs-Calc)/kHz $C_1$ (GG) |
|---|---|---|---|---|---|---|---|---|---|---|---|---|
| a-type | | | | | | | | | | | | |
| 2 | 0 | 2 | | 1 | 0 | 1 | | | | | 7532 | 0.2 |
| 2 | 1 | 2 | | 1 | 1 | 1 | | | | | 7348.578 | 0.7 |
| 2 | 1 | 1 | | 1 | 1 | 0 | | | | | 7730.506 | -0.7 |
| 3 | 0 | 3 | | 2 | 0 | 2 | 10490.083 | 0.2 | | | 11279.15 | -2 |
| 3 | 1 | 3 | | 2 | 1 | 2 | 10224.786 | -2 | | | 11018.2 | -0.3 |
| 3 | 1 | 2 | | 2 | 1 | 1 | 10801.179 | 1.6 | | | 11590.9 | -0.2 |
| 3 | 2 | 2 | | 2 | 2 | 1 | | | | | 11309.21 | 0.6 |
| 3 | 2 | 1 | | 2 | 2 | 0 | | | | | 11339.36 | 1.5 |
| 4 | 0 | 4 | | 3 | 0 | 3 | 13955.418 | 0.8 | | | 15004.14 | 0.3 |
| 4 | 1 | 4 | | 3 | 1 | 3 | 13625.428 | -0.9 | | | 14682.49 | 0.1 |
| 4 | 1 | 3 | | 3 | 1 | 2 | 14393.244 | 0.6 | | | 15445.21 | 0.2 |
| 4 | 2 | 3 | | 3 | 2 | 2 | 14017.6 | 2.5 | | | 15073 | 0 |
| 4 | 2 | 2 | | 3 | 2 | 1 | 14085.16 | -2.3 | | | 15147.88 | -0.4 |
| 5 | 0 | 5 | | 4 | 0 | 4 | 17395.051 | 0.6 | 15762.09 | 0.1 | 18700.97 | 0.8 |
| 5 | 1 | 5 | | 4 | 1 | 4 | 17019.976 | 0 | 15295.2 | -0.1 | 18340.08 | -0.6 |
| 5 | 1 | 4 | | 4 | 1 | 3 | 17977.71 | -0.9 | 16490.98 | -0.9 | 19290.94 | -0.5 |
| 5 | 2 | 4 | | 4 | 2 | 3 | 17513.45 | -1.1 | 15911.6 | -2.5 | 18831.7 | 0.3 |
| 5 | 2 | 3 | | 4 | 2 | 2 | 17647.073 | 1.6 | 16080.23 | -2 | 18979.39 | 0.5 |
| 5 | 3 | 3 | | 4 | 3 | 2 | | | | | 18872.37 | 0.2 |
| 5 | 3 | 2 | | 4 | 3 | 1 | | | | | 18876.29 | -0.9 |
| 6 | 0 | 6 | | 5 | 0 | 5 | | | 18827.51 | 1.2 | | |
| 6 | 1 | 6 | | 5 | 1 | 5 | | | 18333.43 | -0.5 | | |
| 6 | 1 | 5 | | 5 | 1 | 4 | | | 19762.46 | -0.4 | | |
| 6 | 2 | 5 | | 5 | 2 | 4 | | | 19078.16 | -1.8 | | |
| 6 | 2 | 4 | | 5 | 2 | 3 | | | 19367.38 | 0 | | |
| b-type | | | | | | | | | | | | |
| 2 | 1 | 2 | | 1 | 0 | 1 | | | 11034.74 | -0.6 | | |
| 3 | 1 | 3 | | 2 | 0 | 2 | | | 13864.25 | -0.4 | | |
| 4 | 1 | 4 | | 3 | 0 | 3 | | | 16588.14 | 1.3 | | |
| 5 | 1 | 5 | | 4 | 0 | 4 | | | 19224.02 | 2.3 | | |
| 7 | 0 | 7 | | 6 | 1 | 6 | | | 18886.21 | 1.6 | | |
| 3 | 2 | 1 | | 3 | 1 | 2 | | | 14395.5 | -2.8 | | |

| | | | | | | | | | | | | |
|---|---|---|---|---|---|---|---|---|---|---|---|---|
| 4 | 2 | 2 | 4 | 1 | 3 | | | 14011.93 | -1 | | | |
| 3 | 2 | 2 | 3 | 1 | 3 | | | 15792.21 | 5.6 | | | |
| 4 | 2 | 3 | 4 | 1 | 4 | | | 16282.03 | -3.8 | | | |
| 5 | 2 | 4 | 5 | 1 | 5 | | | 16898.44 | 0.8 | | | |
| 6 | 2 | 5 | 6 | 1 | 6 | | | 17643.18 | 5.4 | | | |
| 7 | 2 | 6 | 7 | 1 | 7 | | | 18517.46 | -2.2 | | | |
| 8 | 2 | 7 | 8 | 1 | 8 | | | 19521.64 | -0.1 | | | |
| c-type | | | | | | | | | | | | |
| 2 | 2 | 0 | 1 | 1 | 0 | 19123.904 | 1.7 | | | 18302.72 | -0.3 | |
| 2 | 1 | 1 | 1 | 0 | 1 | 11367.013 | 0.4 | | | 11443.03 | -0.5 | |
| 2 | 2 | 1 | 1 | 1 | 1 | 19309.274 | -1.5 | | | 18486.12 | 0.3 | |
| 3 | 1 | 2 | 2 | 0 | 2 | | | | | 15501.94 | 0.5 | |
| 3 | 2 | 2 | 3 | 1 | 2 | | | 14352.6 | -1.9 | | | |
| 4 | 1 | 3 | 3 | 0 | 3 | 19066.643 | -0.9 | 18986.44 | 0.4 | | | |
| 8 | 0 | 8 | 7 | 1 | 6 | | | 15689.86 | 1.4 | | | |
| 9 | 0 | 9 | 8 | 1 | 7 | | | 17242.54 | 0.8 | | | |
| 10 | 0 | 10 | 9 | 1 | 8 | | | 18525.25 | 1.4 | | | |
| 11 | 0 | 11 | 10 | 1 | 9 | | | 19555.95 | -1.6 | | | |
| 3 | 2 | 1 | 3 | 1 | 3 | | | 15835.1 | -3.5 | | | |
| 4 | 2 | 2 | 4 | 1 | 4 | | | 16410.23 | 0.6 | | | |
| 5 | 2 | 3 | 5 | 1 | 5 | | | 17195.26 | 1.5 | | | |
| 6 | 2 | 4 | 6 | 1 | 6 | | | 18229.21 | 1.7 | | | |
| 7 | 2 | 5 | 7 | 1 | 7 | | | 19551.97 | -1.1 | | | |
| 9 | 1 | 8 | 8 | 2 | 6 | | | 16812.77 | -0.6 | | | |

Supplementary Table 3. Observed transitions of the parent species of perfluoropentane.

| J' | $K_p$' | $K_o$' | ← | J" | $K_p$" | $K_o$" | Freq/MHz | (Obs-Calc)/kHz |
|---|---|---|---|---|---|---|---|---|
| 15 | 1 | 15 | | 14 | 0 | 14 | 9501.7333 | -2.1 |
| 16 | 1 | 16 | | 15 | 0 | 15 | 10079.2387 | -0.8 |
| 17 | 1 | 17 | | 16 | 0 | 16 | 10658.4048 | 0.5 |
| 18 | 1 | 18 | | 17 | 0 | 17 | 11239.5385 | 1.8 |
| 19 | 1 | 19 | | 18 | 0 | 18 | 11822.8472 | 4.5 |
| 20 | 1 | 20 | | 19 | 0 | 19 | 12408.4379 | 5.2 |
| 12 | 2 | 11 | | 11 | 1 | 10 | 9150.1492 | -2.0 |
| 14 | 2 | 13 | | 13 | 1 | 12 | 10271.2176 | -3.6 |
| 15 | 2 | 14 | | 14 | 1 | 13 | 10825.9682 | -3.5 |
| 16 | 2 | 15 | | 15 | 1 | 14 | 11377.2042 | -2.3 |
| 10 | 3 | 8 | | 9 | 2 | 7 | 9568.9728 | -0.4 |
| 10 | 3 | 7 | | 9 | 2 | 8 | 9603.4405 | -0.4 |
| 11 | 3 | 9 | | 10 | 2 | 8 | 10176.1181 | -1.4 |
| 11 | 3 | 8 | | 10 | 2 | 9 | 10227.8421 | -0.4 |
| 13 | 3 | 11 | | 12 | 2 | 10 | 11378.8258 | -1.2 |
| 13 | 3 | 10 | | 12 | 2 | 11 | 11483.1319 | -0.6 |
| 14 | 3 | 12 | | 13 | 2 | 11 | 11973.2179 | -1.8 |
| 14 | 3 | 11 | | 13 | 2 | 12 | 12114.9492 | 0.5 |
| 15 | 3 | 13 | | 14 | 2 | 12 | 12562.2666 | -0.1 |
| 9 | 4 | 6 | | 8 | 3 | 5 | 10334.9445 | -0.2 |

| | | | | | | | |
|---|---|---|---|---|---|---|---|
| 9 | 4 | 5 | 8 | 3 | 6 | 10335.2609 | -0.5 |
| 10 | 4 | 7 | 9 | 3 | 6 | 10952.7512 | 0.0 |
| 10 | 4 | 6 | 9 | 3 | 7 | 10953.3852 | -0.6 |
| 11 | 4 | 7 | 10 | 3 | 8 | 11571.4196 | -0.8 |
| 12 | 4 | 9 | 11 | 3 | 8 | 12187.2985 | -0.2 |
| 12 | 4 | 8 | 11 | 3 | 9 | 12189.3676 | -0.4 |
| 5 | 5 | 1 | 4 | 4 | 0 | 9224.9498 | -0.2 |
| 5 | 5 | 0 | 4 | 4 | 1 | 9224.9498 | -0.2 |
| 6 | 5 | 2 | 5 | 4 | 1 | 9843.3475 | 0.3 |
| 6 | 5 | 1 | 5 | 4 | 2 | 9843.3475 | 0.3 |
| 8 | 5 | 4 | 7 | 4 | 3 | 11080.0891 | 0.1 |
| 8 | 5 | 3 | 7 | 4 | 4 | 11080.0891 | -0.5 |
| 9 | 5 | 5 | 8 | 4 | 4 | 11698.4092 | 0.9 |
| 9 | 5 | 4 | 8 | 4 | 5 | 11698.4092 | -1.0 |
| 10 | 5 | 6 | 9 | 4 | 5 | 12316.6721 | 0.2 |
| 11 | 5 | 7 | 10 | 4 | 6 | 12934.8575 | -2.4 |
| 11 | 5 | 6 | 10 | 4 | 7 | 12934.8723 | 1.1 |
| 12 | 5 | 8 | 11 | 4 | 7 | 13552.9489 | -0.5 |
| 12 | 5 | 7 | 11 | 4 | 8 | 13552.9771 | 3.5 |
| 13 | 5 | 9 | 12 | 4 | 8 | 14170.9148 | 1.0 |
| 13 | 5 | 8 | 12 | 4 | 9 | 14170.9615 | -0.8 |
| 14 | 5 | 10 | 13 | 4 | 9 | 14788.7210 | -1.3 |
| 14 | 5 | 9 | 13 | 4 | 10 | 14788.8155 | 1.4 |
| 6 | 6 | 1 | 5 | 5 | 0 | 11206.2246 | 0.4 |
| 6 | 6 | 0 | 5 | 5 | 1 | 11206.2246 | 0.4 |
| 7 | 6 | 1 | 6 | 5 | 2 | 11824.6235 | 0.5 |
| 7 | 6 | 2 | 6 | 5 | 1 | 11824.6235 | 0.5 |
| 8 | 6 | 3 | 7 | 5 | 3 | 12443.0136 | 0.3 |
| 8 | 6 | 3 | 7 | 5 | 2 | 12443.0136 | 0.3 |
| 9 | 6 | 4 | 8 | 5 | 3 | 13061.3884 | -0.2 |
| 9 | 6 | 3 | 8 | 5 | 4 | 13061.3884 | -0.2 |
| 10 | 6 | 4 | 9 | 5 | 5 | 13679.7426 | 1.7 |
| 10 | 6 | 5 | 9 | 5 | 4 | 13679.7426 | 1.8 |
| 11 | 6 | 6 | 10 | 5 | 5 | 14298.0603 | -0.7 |
| 11 | 6 | 5 | 10 | 5 | 6 | 14298.0603 | -0.7 |
| 12 | 6 | 7 | 11 | 5 | 6 | 14916.3379 | -0.4 |
| 13 | 6 | 8 | 12 | 5 | 7 | 15534.5605 | -0.5 |
| 14 | 6 | 9 | 13 | 5 | 8 | 16152.7153 | -0.4 |
| 15 | 6 | 10 | 14 | 5 | 9 | 16770.7865 | -1.1 |
| 7 | 7 | 0 | 6 | 6 | 1 | 13187.4967 | 0.5 |
| 7 | 7 | 1 | 6 | 6 | 0 | 13187.4967 | 0.5 |
| 8 | 7 | 1 | 7 | 6 | 2 | 13805.8977 | 2.3 |
| 8 | 7 | 2 | 7 | 6 | 1 | 13805.8977 | 2.3 |
| 9 | 7 | 2 | 8 | 6 | 3 | 14424.2882 | -0.4 |
| 9 | 7 | 3 | 8 | 6 | 2 | 14424.2882 | -0.4 |
| 10 | 7 | 3 | 9 | 6 | 4 | 15042.6708 | -0.7 |
| 10 | 7 | 4 | 9 | 6 | 3 | 15042.6708 | -0.7 |
| 11 | 7 | 4 | 10 | 6 | 5 | 15661.0389 | -0.2 |
| 11 | 7 | 5 | 10 | 6 | 4 | 15661.0389 | -0.2 |
| 12 | 7 | 5 | 11 | 6 | 6 | 16279.3847 | -0.8 |

| | | | | | | | |
|---|---|---|---|---|---|---|---|
| 12 | 7 | 6 | 11 | 6 | 5 | 16279.3847 | -0.8 |
| 13 | 7 | 6 | 12 | 6 | 7 | 16897.7055 | 1.5 |
| 13 | 7 | 7 | 12 | 6 | 6 | 16897.7055 | 1.5 |
| 14 | 7 | 7 | 13 | 6 | 8 | 17515.9862 | -0.9 |
| 14 | 7 | 8 | 13 | 6 | 8 | 17515.9862 | -0.9 |
| 8 | 8 | 0 | 7 | 7 | 1 | 15168.7663 | 0.6 |
| 8 | 8 | 1 | 7 | 7 | 0 | 15168.7663 | 0.6 |
| 9 | 8 | 1 | 8 | 7 | 2 | 15787.1648 | 0.2 |
| 9 | 8 | 2 | 8 | 7 | 1 | 15787.1648 | 0.2 |
| 10 | 8 | 2 | 9 | 7 | 3 | 16405.5580 | -1.0 |
| 10 | 8 | 3 | 9 | 7 | 2 | 16405.5580 | -1.0 |
| 11 | 8 | 3 | 10 | 7 | 4 | 17023.9450 | -0.8 |
| 11 | 8 | 4 | 10 | 7 | 3 | 17023.9450 | -0.8 |
| 12 | 8 | 4 | 11 | 7 | 5 | 17642.3219 | 0.5 |
| 12 | 8 | 5 | 11 | 7 | 4 | 17642.3219 | 0.5 |
| 10 | 9 | 1 | 9 | 8 | 2 | 17642.3219 | -0.5 |
| 10 | 9 | 2 | 9 | 8 | 1 | 17642.3219 | -0.5 |
| 16 | 0 | 16 | 15 | 1 | 15 | 9557.3693 | 1.5 |
| 17 | 0 | 17 | 16 | 1 | 16 | 10198.0432 | 2.1 |
| 19 | 0 | 19 | 18 | 1 | 18 | 11471.5378 | 3.1 |
| 20 | 0 | 20 | 19 | 1 | 19 | 12104.2603 | 3.1 |
| 18 | 1 | 17 | 17 | 2 | 16 | 9831.7662 | 0.8 |
| 20 | 1 | 19 | 19 | 2 | 18 | 11212.7181 | -0.9 |
| 21 | 2 | 19 | 20 | 3 | 18 | 10098.3663 | -3.2 |
| 33 | 6 | 27 | 32 | 7 | 26 | 11602.3790 | -1.4 |
| 8 | 8 | 1 | 8 | 7 | 2 | 10221.4960 | 2.9 |
| 8 | 8 | 0 | 8 | 7 | 1 | 10221.4960 | 2.9 |
| 11 | 8 | 4 | 11 | 7 | 5 | 10221.2353 | 2.3 |
| 11 | 8 | 3 | 11 | 7 | 4 | 10221.2353 | 2.3 |
| 12 | 8 | 5 | 12 | 7 | 6 | 10221.0876 | 1.3 |
| 12 | 8 | 4 | 12 | 7 | 5 | 10221.0876 | 1.3 |
| 13 | 8 | 6 | 13 | 7 | 7 | 10220.9005 | 0.4 |
| 13 | 8 | 5 | 13 | 7 | 6 | 10220.9005 | 0.4 |
| 14 | 8 | 7 | 14 | 7 | 8 | 10220.6682 | 0.6 |
| 14 | 8 | 6 | 14 | 7 | 7 | 10220.6682 | 0.6 |
| 15 | 8 | 8 | 15 | 7 | 9 | 10220.3824 | 0.7 |
| 15 | 8 | 7 | 15 | 7 | 8 | 10220.3824 | 0.7 |
| 16 | 8 | 9 | 16 | 7 | 10 | 10220.0347 | -0.2 |
| 16 | 8 | 8 | 16 | 7 | 9 | 10220.0347 | -0.2 |
| 17 | 8 | 10 | 17 | 7 | 11 | 10219.6188 | -0.2 |
| 17 | 8 | 9 | 17 | 7 | 10 | 10219.6188 | -0.1 |
| 18 | 8 | 10 | 18 | 7 | 11 | 10219.1257 | 0.4 |
| 18 | 8 | 11 | 18 | 7 | 12 | 10219.1257 | 0.4 |
| 19 | 8 | 11 | 19 | 7 | 12 | 10218.5446 | -0.1 |
| 19 | 8 | 12 | 19 | 7 | 13 | 10218.5446 | -0.1 |
| 20 | 8 | 12 | 20 | 7 | 13 | 10217.8676 | 0.1 |
| 20 | 8 | 13 | 20 | 7 | 14 | 10217.8676 | 0.1 |
| 21 | 8 | 13 | 21 | 7 | 14 | 10217.0832 | -0.3 |
| 21 | 8 | 14 | 21 | 7 | 15 | 10217.0832 | -0.3 |
| 22 | 8 | 14 | 22 | 7 | 15 | 10216.1811 | -0.8 |

| | | | | | | | |
|---|---|---|---|---|---|---|---|
| 22 | 8 | 15 | 22 | 7 | 16 | 10216.1811 | -0.8 |
| 23 | 8 | 15 | 23 | 7 | 16 | 10215.1513 | -0.1 |
| 23 | 8 | 16 | 23 | 7 | 17 | 10215.1513 | -0.2 |
| 24 | 8 | 16 | 24 | 7 | 17 | 10213.9801 | -0.1 |
| 24 | 8 | 17 | 24 | 7 | 18 | 10213.9801 | -0.2 |
| 25 | 8 | 18 | 25 | 7 | 19 | 10212.6560 | -0.1 |
| 25 | 8 | 17 | 25 | 7 | 18 | 10212.6560 | 0.1 |
| 26 | 8 | 18 | 26 | 7 | 19 | 10211.1649 | -0.5 |
| 26 | 8 | 19 | 26 | 7 | 20 | 10211.1649 | -0.9 |
| 27 | 8 | 19 | 27 | 7 | 20 | 10209.4962 | 0.9 |
| 27 | 8 | 20 | 27 | 7 | 21 | 10209.4962 | 0.3 |
| 28 | 8 | 20 | 28 | 7 | 21 | 10207.6309 | -0.5 |
| 28 | 8 | 21 | 28 | 7 | 22 | 10207.6309 | -1.4 |
| 29 | 8 | 21 | 29 | 7 | 22 | 10205.5601 | 1.1 |
| 29 | 8 | 22 | 29 | 7 | 23 | 10205.5601 | -0.3 |
| 30 | 8 | 22 | 30 | 7 | 23 | 10203.2626 | 0.0 |
| 30 | 8 | 23 | 30 | 7 | 24 | 10203.2626 | -2.3 |
| 31 | 8 | 23 | 31 | 7 | 24 | 10200.7253 | -0.9 |
| 31 | 8 | 24 | 31 | 7 | 25 | 10200.7253 | -4.5 |
| 10 | 9 | 2 | 10 | 8 | 3 | 11584.3036 | 0.8 |
| 10 | 9 | 1 | 10 | 8 | 2 | 11584.3036 | 0.8 |
| 11 | 9 | 2 | 11 | 8 | 3 | 11584.2242 | -1.4 |
| 11 | 9 | 3 | 11 | 8 | 4 | 11584.2242 | -1.4 |
| 12 | 9 | 3 | 12 | 8 | 4 | 11584.1246 | -0.9 |
| 12 | 9 | 4 | 12 | 8 | 5 | 11584.1246 | -0.9 |
| 13 | 9 | 4 | 13 | 8 | 5 | 11583.9995 | 1.0 |
| 13 | 9 | 5 | 13 | 8 | 6 | 11583.9995 | 1.0 |
| 14 | 9 | 5 | 14 | 8 | 6 | 11583.8406 | 0.6 |
| 14 | 9 | 6 | 14 | 8 | 7 | 11583.8406 | 0.6 |
| 15 | 9 | 6 | 15 | 8 | 7 | 11583.6457 | 0.5 |
| 15 | 9 | 7 | 15 | 8 | 8 | 11583.6457 | 0.5 |
| 16 | 9 | 7 | 16 | 8 | 8 | 11583.4081 | -0.8 |
| 16 | 9 | 8 | 16 | 8 | 9 | 11583.4081 | -0.8 |
| 17 | 9 | 8 | 17 | 8 | 9 | 11583.1257 | 0.1 |
| 17 | 9 | 9 | 17 | 8 | 10 | 11583.1257 | 0.1 |
| 18 | 9 | 9 | 18 | 8 | 10 | 11582.7896 | 0.1 |
| 18 | 9 | 10 | 18 | 8 | 11 | 11582.7896 | 0.1 |
| 19 | 9 | 10 | 19 | 8 | 11 | 11582.3945 | 0.2 |
| 19 | 9 | 11 | 19 | 8 | 12 | 11582.3945 | 0.2 |
| 20 | 9 | 11 | 20 | 8 | 12 | 11581.9336 | 0.1 |
| 20 | 9 | 12 | 20 | 8 | 13 | 11581.9336 | 0.1 |
| 21 | 9 | 13 | 21 | 8 | 14 | 11581.4000 | -0.1 |
| 21 | 9 | 12 | 21 | 8 | 13 | 11581.4000 | -0.1 |
| 22 | 9 | 13 | 22 | 8 | 14 | 11580.7866 | -0.3 |
| 22 | 9 | 14 | 22 | 8 | 15 | 11580.7866 | -0.3 |
| 23 | 9 | 14 | 23 | 8 | 15 | 11580.0856 | -0.6 |
| 23 | 9 | 15 | 23 | 8 | 16 | 11580.0856 | -0.6 |
| 24 | 9 | 15 | 24 | 8 | 16 | 11579.2896 | -0.4 |
| 24 | 9 | 16 | 24 | 8 | 17 | 11579.2896 | -0.4 |
| 25 | 9 | 16 | 25 | 8 | 17 | 11578.3895 | -0.5 |

| | | | | | | | |
|---|---|---|---|---|---|---|---|
| 25 | 9 | 17 | 25 | 8 | 18 | 11578.3895 | -0.5 |
| 26 | 9 | 17 | 26 | 8 | 18 | 11577.3765 | -1.0 |
| 26 | 9 | 18 | 26 | 8 | 19 | 11577.3765 | -1.0 |
| 27 | 9 | 18 | 27 | 8 | 19 | 11576.2424 | -0.9 |
| 27 | 9 | 19 | 27 | 8 | 20 | 11576.2424 | -0.9 |
| 28 | 9 | 19 | 28 | 8 | 20 | 11574.9765 | -1.5 |
| 28 | 9 | 20 | 28 | 8 | 21 | 11574.9765 | -1.5 |
| 29 | 9 | 20 | 29 | 8 | 21 | 11573.5709 | -0.8 |
| 29 | 9 | 21 | 29 | 8 | 22 | 11573.5709 | -0.8 |
| 30 | 9 | 21 | 30 | 8 | 22 | 11572.0136 | -0.6 |
| 30 | 9 | 22 | 30 | 8 | 23 | 11572.0136 | -0.6 |
| 31 | 9 | 23 | 31 | 8 | 24 | 11570.2941 | -0.9 |
| 31 | 9 | 22 | 31 | 8 | 23 | 11570.2941 | -0.8 |
| 32 | 9 | 23 | 32 | 8 | 24 | 11568.4022 | -0.5 |
| 32 | 9 | 24 | 32 | 8 | 25 | 11568.4022 | -0.6 |
| 33 | 9 | 24 | 33 | 8 | 25 | 11566.3260 | -0.3 |
| 33 | 9 | 25 | 33 | 8 | 26 | 11566.3260 | -0.4 |
| 34 | 9 | 25 | 34 | 8 | 26 | 11564.0537 | 0.1 |
| 34 | 9 | 26 | 34 | 8 | 27 | 11564.0537 | -0.2 |
| 35 | 9 | 26 | 35 | 8 | 27 | 11561.5727 | 0.1 |
| 35 | 9 | 27 | 35 | 8 | 28 | 11561.5727 | -0.3 |
| 36 | 9 | 27 | 36 | 8 | 28 | 11558.8707 | 0.3 |
| 36 | 9 | 28 | 36 | 8 | 29 | 11558.8707 | -0.3 |
| 37 | 9 | 28 | 37 | 8 | 29 | 11555.9350 | 1.2 |
| 37 | 9 | 29 | 37 | 8 | 30 | 11555.9350 | 0.2 |
| 38 | 9 | 29 | 38 | 8 | 30 | 11552.7510 | 1.8 |
| 38 | 9 | 30 | 38 | 8 | 31 | 11552.7510 | 0.2 |
| 39 | 9 | 30 | 39 | 8 | 31 | 11549.3047 | 2.2 |
| 39 | 9 | 31 | 39 | 8 | 32 | 11549.3047 | -0.2 |
| 40 | 9 | 31 | 40 | 8 | 32 | 11545.5845 | 5.5 |
| 40 | 9 | 32 | 40 | 8 | 33 | 11545.5845 | 1.9 |

Supplementary Table 4. Observed transitions for the three $^{13}C$ isotopomers of perfluoropentane.

| | | | | | | | $^{13}C_1$ | $^{13}C_1$ | $^{13}C_2$ | $^{13}C_2$ | $^{13}C_3$ | $^{13}C_3$ |
|---|---|---|---|---|---|---|---|---|---|---|---|---|
| J' | Kp' | Ko' | ← | J" | Kp" | Ko" | Freq/MHz | (Obs-Calc)/kHz | Freq/MHz | (Obs-Calc)/kHz | Freq/MHz | (Obs-Calc)/kHz |
| 6 | 5 | 2 | | 5 | 4 | 1 | 9838.4135 | 1.9 | 9837.4304 | -2.0 | | |
| 6 | 5 | 1 | | 5 | 4 | 2 | 9838.4135 | 1.9 | 9837.4304 | -2.0 | | |
| 6 | 6 | 1 | | 5 | 5 | 0 | 11203.6076 | 0.7 | 11199.8615 | -0.1 | | |
| 6 | 6 | 0 | | 5 | 5 | 1 | 11203.6076 | 0.7 | 11199.8615 | -0.1 | | |
| 9 | 6 | 4 | | 8 | 5 | 3 | 13051.0890 | 1.4 | | | 13059.2684 | 2.9 |
| 9 | 6 | 3 | | 8 | 5 | 4 | 13051.0890 | 1.4 | | | 13059.2684 | 2.9 |
| 10 | 6 | 5 | | 9 | 5 | 4 | 13666.8802 | 0.9 | | | 13677.6292 | -0.1 |
| 10 | 6 | 4 | | 9 | 5 | 5 | 13666.8802 | 0.9 | | | 13677.6292 | -0.1 |
| 11 | 6 | 6 | | 10 | 5 | 5 | 14282.6395 | 0.3 | | | 14295.9610 | 0.3 |
| 11 | 6 | 5 | | 10 | 5 | 6 | 14282.6395 | 0.2 | | | 14295.9610 | 0.3 |
| 12 | 6 | 7 | | 11 | 5 | 6 | 14898.3562 | -0.9 | | | 14914.2488 | -0.3 |

| | | | | | | | | | | | |
|---|---|---|---|---|---|---|---|---|---|---|---|
| 12 | 6 | 6 | 11 | 5 | 7 | 14898.3562 | -1.0 | | | 14914.2488 | -0.5 |
| 13 | 6 | 8 | 12 | 5 | 7 | 15514.0220 | 0.9 | | | 15532.4793 | -3.4 |
| 13 | 6 | 7 | 12 | 5 | 8 | 15514.0220 | 0.6 | | | 15532.4793 | -3.7 |
| 7 | 7 | 1 | 6 | 6 | 0 | 13184.6361 | 0.2 | | | | |
| 7 | 7 | 0 | 6 | 6 | 1 | 13184.6361 | 0.2 | | | | |
| 8 | 7 | 2 | 7 | 6 | 1 | 13800.4721 | -1.6 | | | | |
| 8 | 7 | 1 | 7 | 6 | 2 | 13800.4721 | -1.6 | | | | |
| 9 | 7 | 3 | 8 | 6 | 2 | 14416.3029 | -2.7 | | | 14421.7632 | 2.6 |
| 9 | 7 | 2 | 8 | 6 | 3 | 14416.3029 | -2.7 | | | 14421.7632 | 2.6 |
| 10 | 7 | 4 | 9 | 6 | 3 | 15032.1310 | 3.6 | | | 15040.1537 | -1.5 |
| 10 | 7 | 3 | 9 | 6 | 4 | 15032.1310 | 3.6 | | | 15040.1537 | -1.5 |
| 11 | 7 | 5 | 10 | 6 | 4 | 15647.9372 | 3.2 | | | | |
| 11 | 7 | 4 | 10 | 6 | 5 | 15647.9372 | 3.2 | | | | |
| 8 | 8 | 1 | 7 | 7 | 0 | 15165.6611 | -1.4 | 15160.2088 | 1.0 | | |
| 8 | 8 | 0 | 7 | 7 | 1 | 15165.6611 | -1.4 | 15160.2088 | 1.0 | | |
| 9 | 8 | 2 | 8 | 7 | 1 | 15781.5008 | 0.8 | 15777.9564 | -0.3 | | |
| 9 | 8 | 1 | 8 | 7 | 2 | 15781.5008 | 0.8 | 15777.9564 | -0.3 | | |
| 10 | 8 | 3 | 9 | 7 | 2 | 16397.3325 | -0.5 | 16395.7019 | 0.8 | | |
| 10 | 8 | 2 | 9 | 7 | 3 | 16397.3325 | -0.5 | 16395.7019 | 0.8 | | |
| 9 | 9 | 1 | 8 | 8 | 0 | 17146.6840 | -2.2 | | | | |
| 9 | 9 | 0 | 8 | 8 | 1 | 17146.6840 | -2.2 | | | | |
| | | | | | | | | | | | |
| 13 | 1 | 13 | 12 | 0 | 12 | 8319.9113 | 1.9 | 8340.5858 | 0.1 | | |
| 9 | 3 | 7 | 8 | 2 | 6 | 8941.7249 | -4.4 | 8951.7224 | 0.2 | 8957.7913 | -0.2 |
| 9 | 3 | 6 | 8 | 2 | 7 | 8963.2874 | -1.1 | 8973.7438 | -0.9 | 8979.8019 | -0.6 |
| 10 | 3 | 8 | 9 | 2 | 7 | 9549.5015 | -0.4 | 9561.2360 | -0.3 | 9567.9715 | -0.4 |
| 10 | 3 | 7 | 9 | 2 | 8 | 9583.4261 | -0.3 | 9595.8912 | 2.4 | 9602.6034 | -1.1 |
| 11 | 3 | 9 | 10 | 2 | 8 | 10154.2590 | -0.3 | 10167.6726 | -1.5 | 10175.0796 | 2.0 |
| 11 | 3 | 8 | 10 | 2 | 9 | 10205.1685 | -0.5 | 10219.6737 | -0.1 | | |
| 12 | 3 | 10 | 11 | 2 | 9 | 10755.4071 | 0.0 | 10770.4315 | -0.2 | 10778.5057 | 0.6 |
| 12 | 3 | 9 | 11 | 2 | 10 | 10828.8964 | 1.8 | 10845.4868 | -0.1 | 10853.5203 | 3.1 |
| 13 | 3 | 11 | 12 | 2 | 10 | 11352.3501 | -2.9 | 11368.9093 | 0.9 | | |
| 10 | 4 | 7 | 9 | 3 | 6 | 10935.2739 | -1.3 | 10944.6771 | 0.7 | 10951.4384 | -4.5 |
| 10 | 4 | 6 | 9 | 3 | 7 | 10935.8967 | 2.3 | 10945.3149 | -1.4 | 10952.0826 | 0.4 |

Supplementary Table 5. Assigned rotational transitions of perfluorohexane.

| J' | $K_p$' | $K_o$' | ← | J" | $K_p$" | $K_o$" | Freq/MHz | (Obs-Calc)/kHz |
|---|---|---|---|---|---|---|---|---|
| 9 | 3 | 6 | | 8 | 2 | 6 | 6725.7069 | 0.4 |
| 9 | 3 | 7 | | 8 | 2 | 7 | 6729.4562 | -0.1 |
| 10 | 3 | 7 | | 9 | 2 | 7 | 7124.8484 | 0.1 |
| 10 | 3 | 8 | | 9 | 2 | 8 | 7130.7216 | -0.7 |
| 11 | 3 | 8 | | 10 | 2 | 8 | 7523.4590 | 3.2 |
| 11 | 3 | 9 | | 10 | 2 | 9 | 7532.2333 | -1.3 |
| 12 | 3 | 9 | | 11 | 2 | 9 | 7921.4137 | -1.9 |
| 12 | 3 | 10 | | 11 | 2 | 10 | 7934.0424 | -0.4 |
| 13 | 3 | 10 | | 12 | 2 | 10 | 8318.6058 | -1.3 |

| | | | | | | | |
|---|---|---|---|---|---|---|---|
| 13 | 3 | 11 | 12 | 2 | 11 | 8336.1984 | -1.3 |
| 14 | 3 | 11 | 13 | 2 | 11 | 8714.9045 | -0.2 |
| 14 | 3 | 12 | 13 | 2 | 12 | 8736.7617 | 0.2 |
| 15 | 3 | 12 | 14 | 2 | 12 | 9110.1776 | -2.1 |
| 15 | 3 | 13 | 14 | 2 | 13 | 9141.7876 | 0.0 |
| 16 | 3 | 13 | 15 | 2 | 13 | 9504.3024 | -1.4 |
| 16 | 3 | 14 | 15 | 2 | 14 | 9545.3385 | -1.4 |
| 17 | 3 | 14 | 16 | 2 | 14 | 9897.1512 | -0.1 |
| 17 | 3 | 15 | 16 | 2 | 15 | 9949.4838 | 1.2 |
| 18 | 3 | 15 | 17 | 2 | 15 | 10288.6014 | -2.0 |
| 18 | 3 | 16 | 17 | 2 | 16 | 10354.2831 | 1.1 |
| 19 | 3 | 16 | 18 | 2 | 16 | 10678.5520 | 0.6 |
| 20 | 3 | 17 | 19 | 2 | 17 | 11066.9008 | 0.1 |
| 8 | 4 | 4 | 7 | 3 | 4 | 7576.7595 | -3.0 |
| 8 | 4 | 5 | 7 | 3 | 5 | 7576.7758 | 2.3 |
| 9 | 4 | 5 | 8 | 3 | 5 | 7977.2669 | 1.0 |
| 9 | 4 | 6 | 8 | 3 | 6 | 7977.2877 | -2.4 |
| 10 | 4 | 6 | 9 | 3 | 6 | 8377.7427 | 6.7 |
| 10 | 4 | 7 | 9 | 3 | 7 | 8377.7834 | -1.0 |
| 11 | 4 | 7 | 10 | 3 | 7 | 8778.1587 | -2.8 |
| 11 | 4 | 8 | 10 | 3 | 8 | 8778.2535 | 2.3 |
| 12 | 4 | 8 | 11 | 3 | 8 | 9178.5277 | -0.8 |
| 12 | 4 | 9 | 11 | 3 | 9 | 9178.6851 | -0.2 |
| 5 | 5 | 0 | 4 | 4 | 0 | 7624.3825 | 1.7 |
| 5 | 5 | 1 | 4 | 4 | 1 | 7624.3825 | 1.7 |
| 6 | 5 | 1 | 5 | 4 | 1 | 8024.9404 | 0.3 |
| 6 | 5 | 2 | 5 | 4 | 2 | 8024.9404 | 0.3 |
| 7 | 5 | 2 | 6 | 4 | 2 | 8425.4977 | 0.8 |
| 7 | 5 | 3 | 6 | 4 | 3 | 8425.4977 | 0.8 |
| 8 | 5 | 3 | 7 | 4 | 3 | 8826.0487 | -0.4 |
| 8 | 5 | 4 | 7 | 4 | 4 | 8826.0487 | -0.4 |
| 9 | 5 | 4 | 8 | 4 | 4 | 9226.5934 | -0.8 |
| 9 | 5 | 5 | 8 | 4 | 5 | 9226.5934 | -0.9 |
| 10 | 5 | 5 | 9 | 4 | 5 | 9627.1285 | -0.9 |
| 10 | 5 | 6 | 9 | 4 | 6 | 9627.1285 | -1.0 |
| 11 | 5 | 6 | 10 | 4 | 6 | 10027.6491 | -2.1 |
| 11 | 5 | 7 | 10 | 4 | 7 | 10027.6491 | -2.4 |

Supplementary Table 6. Observed and assigned transitions for the gauche and trans conformers of 1H-heptafluoropropane.

| | | | | | | | Gauche | Gauche (Obs-Calc)/kHz | Trans | Trans (Obs-Calc)/kHz |
|---|---|---|---|---|---|---|---|---|---|---|
| J' | $K_p$' | $K_o$' | ← | J'' | $K_p$'' | $K_o$'' | Freq/MHz | | Freq/MHz | |
| a-types | | | | | | | | | | |
| 4 | 0 | 4 | | 3 | 0 | 3 | 8271.8813 | 0.4 | 9257.7763 | -0.1 |
| 5 | 0 | 5 | | 4 | 0 | 4 | 10257.4942 | -3.6 | 11553.0458 | -0.8 |
| 6 | 0 | 6 | | 5 | 0 | 5 | 12219.2199 | 0.4 | | |

| | | | | | | | | | |
|---|---|---|---|---|---|---|---|---|---|
| 7 | 0 | 7 | 6 | 0 | 6 | 14171.5208 | 0.4 | | |
| 4 | 1 | 3 | 3 | 1 | 2 | | | 9374.1207 | -0.5 |
| 5 | 1 | 4 | 4 | 1 | 3 | | | 11711.5802 | -0.3 |
| 4 | 1 | 4 | 3 | 1 | 3 | 8109.8122 | 0.1 | | |
| 5 | 1 | 5 | 4 | 1 | 4 | 10115.4563 | 0.0 | | |
| 6 | 1 | 6 | 5 | 1 | 5 | 12110.9545 | 0.9 | | |
| 7 | 1 | 7 | 6 | 1 | 6 | 14097.5409 | -0.1 | | |
| 4 | 2 | 2 | 3 | 2 | 1 | | | 9311.0208 | 0.7 |
| 5 | 2 | 3 | 4 | 2 | 2 | | | 11654.3509 | 0.4 |
| 4 | 2 | 3 | 3 | 2 | 1 | | | 9283.2838 | 0.5 |
| 5 | 2 | 4 | 4 | 2 | 3 | | | 11600.5447 | 0.0 |
| 4 | 3 | 2 | 3 | 3 | 1 | | | 9290.8261 | 0.3 |
| 5 | 3 | 3 | 4 | 3 | 2 | | | 11615.4784 | -0.3 |
| 3 | 2 | 1 | 2 | 0 | 2 | | | 9348.2797 | -2.6 |
| 4 | 2 | 2 | 3 | 0 | 3 | | | 11706.4242 | 1.1 |
| b-types | | | | | | | | | |
| 4 | 1 | 4 | 3 | 0 | 3 | | | 9647.7934 | 1.1 |
| 5 | 1 | 5 | 4 | 0 | 4 | | | 11867.2882 | -0.1 |
| 3 | 2 | 1 | 2 | 1 | 2 | 9420.9505 | -1.2 | | |
| 4 | 2 | 2 | 3 | 1 | 3 | 11867.5765 | 1.0 | 11244.1661 | 0.3 |
| 5 | 2 | 3 | 4 | 1 | 4 | | | 13712.9829 | 1.6 |
| 3 | 2 | 2 | 2 | 1 | 1 | 8934.5772 | 0.7 | | |
| 4 | 2 | 3 | 3 | 1 | 2 | 10829.4948 | 0.3 | 10918.5964 | -1.2 |
| 5 | 2 | 4 | 4 | 1 | 3 | | | 13145.0215 | 0.3 |
| 3 | 3 | 1 | 2 | 2 | 0 | 11022.7468 | 0.8 | 9922.0559 | 1.0 |
| 4 | 3 | 2 | 3 | 2 | 1 | 13094.1046 | -0.8 | 12237.4867 | -1.0 |
| 3 | 3 | 0 | 2 | 2 | 1 | 11038.7443 | -1.1 | 9924.9952 | 0.7 |
| 4 | 3 | 1 | 3 | 2 | 2 | 13174.9626 | -0.7 | 12252.3286 | -1.2 |
| 11 | 9 | 2 | 10 | 8 | 3 | | | 10047.9244 | 1.4 |
| 12 | 9 | 3 | 11 | 8 | 4 | | | 10044.9070 | 1.3 |
| 13 | 9 | 4 | 12 | 8 | 5 | | | 10041.1173 | 3.0 |
| 14 | 9 | 5 | 13 | 8 | 6 | | | 10036.4164 | -4.6 |
| 4 | 0 | 4 | 3 | 1 | 3 | 7675.7466 | 0.3 | | |
| 5 | 0 | 5 | 4 | 1 | 4 | 9823.4325 | 0.4 | 11163.0289 | -1.8 |
| 6 | 0 | 6 | 5 | 1 | 5 | 11927.1952 | 0.0 | 13524.3707 | -1.0 |
| 5 | 1 | 4 | 4 | 2 | 3 | 8606.5753 | -0.3 | 10167.1039 | -0.2 |
| 6 | 1 | 5 | 5 | 2 | 4 | 11006.6988 | 0.0 | 12610.9590 | -0.6 |
| 6 | 2 | 4 | 5 | 3 | 3 | 8576.4345 | 0.0 | 11117.3594 | 0.6 |
| 7 | 2 | 5 | 6 | 3 | 4 | 11051.1536 | -0.8 | 13537.0984 | -1.2 |
| 6 | 3 | 3 | 5 | 4 | 2 | | | 9814.3443 | 0.9 |
| 7 | 3 | 4 | 6 | 4 | 3 | | | 12156.4483 | 0.3 |
| 7 | 4 | 3 | 6 | 5 | 2 | | | 10945.9649 | 0.3 |
| 8 | 4 | 4 | 7 | 5 | 3 | | | 13227.7959 | -1.1 |
| 8 | 6 | 2 | 7 | 7 | 1 | | | 10894.9202 | 4.8 |
| 9 | 6 | 3 | 8 | 7 | 2 | | | 13221.5676 | -2.0 |
| 10 | 6 | 5 | 10 | 5 | 6 | 10265.9605 | 0.5 | | |
| 11 | 6 | 6 | 11 | 5 | 7 | 10226.6561 | 0.2 | | |
| 12 | 6 | 7 | 12 | 5 | 8 | 10179.8824 | 0.3 | | |
| c-types | | | | | | | | | |
| 3 | 1 | 2 | 2 | 0 | 2 | 7670.6820 | 1.1 | | |

| | | | | | | | |
|---|---|---|---|---|---|---|---|
| 4 | 1 | 3 | 3 | 0 | 3 | 10074.3087 | 0.0 |
| 4 | 2 | 2 | 3 | 1 | 2 | 11043.3012 | 0.3 |
| 5 | 2 | 3 | 4 | 1 | 3 | 13128.2254 | 0.1 |
| 3 | 2 | 2 | 2 | 1 | 2 | 9347.2279 | 0.0 |
| 4 | 2 | 3 | 3 | 1 | 3 | 11653.7700 | 0.9 |
| 3 | 3 | 0 | 2 | 2 | 0 | 11023.7700 | -2.0 |
| 4 | 3 | 1 | 3 | 2 | 1 | 13101.2391 | -0.4 |
| 3 | 3 | 1 | 2 | 2 | 1 | 11037.7213 | 2.0 |
| 4 | 3 | 2 | 3 | 2 | 2 | 13167.8296 | 0.4 |
| 7 | 0 | 7 | 6 | 1 | 5 | 11181.7455 | 0.0 |
| 8 | 0 | 8 | 7 | 1 | 6 | 12360.9606 | 0.1 |
| 7 | 1 | 7 | 6 | 2 | 5 | 9747.0534 | -1.3 |
| 8 | 1 | 8 | 7 | 2 | 6 | 11217.2498 | 1.4 |
| 7 | 2 | 5 | 6 | 3 | 3 | 10968.6913 | 0.2 |
| 8 | 2 | 6 | 7 | 3 | 4 | 13392.1149 | -0.3 |
| 7 | 2 | 6 | 6 | 3 | 4 | 9640.9176 | -0.5 |
| 8 | 2 | 7 | 7 | 3 | 5 | 11498.0450 | 0.1 |
| 6 | 6 | 1 | 6 | 5 | 1 | 10348.3078 | -1.8 |
| 7 | 6 | 2 | 7 | 5 | 2 | 10336.9126 | -1.0 |
| 8 | 6 | 3 | 8 | 5 | 3 | 10319.6089 | 0.2 |
| 9 | 6 | 4 | 9 | 5 | 4 | 10294.1767 | 0.9 |
| 10 | 6 | 5 | 10 | 5 | 5 | 10257.3890 | -1.0 |
| 11 | 6 | 6 | 11 | 5 | 6 | 10204.3173 | -0.2 |
| 12 | 6 | 7 | 12 | 5 | 7 | 10127.2570 | 0.1 |
| 13 | 6 | 8 | 13 | 5 | 8 | 10014.3781 | -1.5 |
| 14 | 6 | 9 | 14 | 5 | 9 | 9848.4528 | 0.0 |
| 15 | 6 | 10 | 15 | 5 | 10 | 9606.6497 | -0.6 |
| 6 | 6 | 0 | 6 | 5 | 2 | 10348.3440 | 1.5 |
| 7 | 6 | 1 | 7 | 5 | 3 | 10337.1090 | -1.9 |
| 8 | 6 | 2 | 8 | 5 | 4 | 10320.4614 | -0.4 |
| 9 | 6 | 3 | 9 | 5 | 5 | 10297.1463 | 0.9 |
| 10 | 6 | 4 | 10 | 5 | 6 | 10266.2175 | 1.4 |
| 11 | 6 | 5 | 11 | 5 | 7 | 10227.5176 | 1.1 |
| 12 | 6 | 6 | 12 | 5 | 8 | 10182.4249 | 0.7 |
| 13 | 6 | 7 | 13 | 5 | 9 | 10134.8843 | 0.5 |
| 14 | 6 | 8 | 14 | 5 | 10 | 10092.7006 | 3.5 |
| 15 | 6 | 9 | 15 | 5 | 11 | 10068.9828 | -2.4 |
| 16 | 6 | 10 | 16 | 5 | 12 | 10083.6851 | -0.7 |
| 6 | 0 | 6 | 5 | 1 | 4 | 9892.1192 | 0.4 |
| 7 | 0 | 7 | 6 | 1 | 5 | 11181.7450 | -0.5 |
| 9 | 5 | 5 | 8 | 6 | 3 | 8704.5955 | 0.8 |
| 10 | 5 | 6 | 9 | 6 | 4 | 10860.7858 | -0.6 |
| 9 | 5 | 4 | 8 | 6 | 2 | 8707.5955 | 0.1 |
| 10 | 5 | 5 | 9 | 6 | 3 | 10869.2914 | -0.4 |

Supplementary Table 7. Observed transitions of perfluoropropane.

| J' | $K_p$' | $K_o$' | ← | J'' | $K_p$'' | $K_o$'' | Freq/MHz | (Obs-Calc)/kHz |
|---|---|---|---|---|---|---|---|---|
| 3 | 1 | 3 | | 2 | 0 | 2 | 6153.1985 | -0.2 |
| 4 | 1 | 4 | | 3 | 0 | 3 | 7904.7635 | -0.6 |
| 5 | 1 | 5 | | 4 | 0 | 4 | 9640.0275 | 0.0 |
| 3 | 2 | 2 | | 2 | 1 | 1 | 7736.3745 | 0.3 |
| 5 | 2 | 4 | | 4 | 1 | 3 | 11253.6880 | 0.9 |
| 3 | 3 | 1 | | 2 | 2 | 0 | 9319.5531 | 0.1 |
| 3 | 3 | 0 | | 2 | 2 | 1 | 9322.6897 | -0.1 |
| 4 | 3 | 2 | | 3 | 2 | 1 | 11168.7505 | -0.1 |
| 5 | 3 | 3 | | 4 | 2 | 2 | 13006.1924 | -1.1 |
| 5 | 3 | 2 | | 4 | 2 | 3 | 13053.9871 | 0.8 |
| 4 | 4 | 1 | | 3 | 3 | 0 | 12678.3325 | 0.0 |
| 5 | 4 | 2 | | 4 | 3 | 1 | 14534.1711 | -0.7 |
| 5 | 4 | 1 | | 4 | 3 | 2 | 14534.9288 | 0.4 |
| 5 | 5 | 0 | | 4 | 4 | 1 | 16035.5838 | 0.2 |
| 4 | 0 | 4 | | 3 | 1 | 3 | 6793.5592 | 0.6 |
| 5 | 0 | 5 | | 4 | 1 | 4 | 8707.0240 | -0.4 |

The following four transitions were measured for the $^{13}C_1$ isotopomer.

| | | | | | | | | |
|---|---|---|---|---|---|---|---|---|
| 5 | 3 | 3 | | 4 | 2 | 2 | 12990.7842 | 0 |
| 4 | 4 | 1 | | 3 | 3 | 0 | 12673.7949 | -3.4 |
| 4 | 4 | 0 | | 3 | 3 | 1 | 12673.8979 | 3.4 |
| 5 | 4 | 1 | | 4 | 3 | 2 | 14523.7950 | 0 |

| | |
|---|---|
| A/MHz | 1678.4191(8) |
| B/MHz | 951.160(9) |
| C/MHz | 897.850(4) |
| $D_k$/kHz | [0.15][a] |

[a] held fixed at parent value.